KUOPION YLIOPISTON JULKAISUJA C. LUONNONTIETEET JA YMPÄRISTÖTIETEET 226
KUOPIO UNIVERSITY PUBLICATIONS C. NATURAL AND ENVIRONMENTAL SCIENCES 226

JANNE HUTTUNEN

Approximation and Modelling Errors in Nonstationary Inverse Problems

Doctoral dissertation

To be presented by permission of the Faculty of Natural and Environmental Sciences
of the University of Kuopio for public examination in Auditorium ML3,
Medistudia building, University of Kuopio,
on Friday 25th January 2008, at 1 p.m.

Department of Physics
University of Kuopio

KUOPION YLIOPISTO

KUOPIO 2008

Distributor: Kuopio University Library
P.O. Box 1627
FI-70211 KUOPIO
FINLAND
Tel. +358 17 163 430
Fax +358 17 163 410
http://www.uku.fi/kirjasto/julkaisutoiminta/julkmyyn.html

Series Editors: Professor Pertti Pasanen, Ph.D.
Department of Environmental Science

Professor Jari Kaipio, Ph.D.
Department of Physics

Author's address: Department of Physics
University of Kuopio
P.O. Box 1627
FI-70211 KUOPIO
FINLAND
Tel. +358 17 162 495
Fax +358 17 162 585
E-mail: Janne.Huttunen@uku.fi

Supervisor: Professor Jari Kaipio, Ph.D.
Department of Physics
University of Kuopio

Reviewers: Professor Matti Lassas, Ph.D.
Institute of Mathematics
Helsinki University of Technology

Tuomo Kauranne, Ph.D.
Department of Mathematics
Lappeenranta University of Technology

Opponent: Professor Heikki Haario
Department of Mathematics
Lappeenranta University of Technology

ISBN 978-951-27-0964-9
ISBN 978-951-27-0799-7 (PDF)
ISSN 1235-0486

Kopijyvä
Kuopio 2008
Finland

Huttunen, Janne. Approximation and modelling errors in nonstationary inverse problems. Kuopio University Publications C. Natural and Environmental Sciences 226. 2008. 56 p.
ISBN 978-951-27-0964-9
ISBN 978-951-27-0799-7 (PDF)
ISSN 1235-0486

ABSTRACT

Inverse problems usually understood as tasks in which a quantity of interest (e.g., model parameters or shape of the target) is determined based on indirect observations. In this thesis we consider nonstationary inverse problems, i.e., problems in which the unknown quantity is time-varying.

Inverse problems are usually ill-posed which means that the problem has no unique or stable solution. Due to the ill-posedness of the problem, the required accuracy for the state space representation is high. However, in several practical problems an adequately accurate state space form can be computationally very demanding leading to excessively long computational time. Thus the approximative reduced order models have to be used. However, reduced accuracy in the forward model can compromise the quality of computed estimates.

The reduced accuracy of the models can be handled by using so-called approximation error theory. In this approach, the errors related to the approximation are analyzed statistically and this statistical information is used in the solution of the estimation problem.

In this thesis we develop approximation error methods for nonstationary inverse problems. We cast the problems in the state space formalism and analyze the approximation errors in the associated state space models. In addition, we extend the well known Kalman filter recursion to accommodate approximation error models. Both linear and nonlinear state space representations are considered.

As applications, we consider four different problems in which the uncertainties caused by numerical discretization are analyzed. More specifically, first, we predict the temperature evolution in a one–dimensional rod, and second, we consider concentration distribution monitoring in a one–dimensional pipe. The last two applications are related to parameter identification problems (problem in which unknown parameters in the associated model are estimated). We estimate the coefficients of the one–dimensional thermal equation and, as the last problem, we consider the determination of heterogeneous thermal conductivity and a perfusion related coefficient by using ultrasound induced heating and MR temperature measurements.

AMS (MOS) Classification: 35R30, 37M99, 93E11, 65J22
PACS Classification: 02.30.Zz, 02.60.Lj
Universal Decimal Classification: 517.972.7, 53.088, 681.5.015.44
INSPEC Thesaurus: inverse problems; time-varying systems; approximation theory; modelling; errors; error analysis; state-space methods; state estimation; Kalman filters; thermal variables measurement

Acknowledgements

This work was carried out in the Department of Physics, University of Kuopio, during the years 2003–2007. The study was financially supported by the Academy of Finland and the Finnish Funding Agency for Technology and Innovation (TEKES).

I want to express my warmest gratitude to my supervisor Professor Jari Kaipio, Ph.D., for providing guidance during all these years. I am also very grateful to my co-authors Hanna-Katriina Pikkarainen, Ph.D., Matti Malinen, Ph.D., and Tomi Huttunen, Ph.D., for the fruitful collaboration during this work.

I wish to thank the official reviewers Professor Matti Lassas, Ph.D., and Tuomo Kauranne, Ph.D., for carefully reading the manuscript and giving valuable suggestions for the thesis.

I would like to thank the staff of the Department of Physics at the University of Kuopio for their support. Especially, I want to thank all my co-workers in the Inverse Problems Group. A special thank goes to Olli-Pekka Tossavainen, Ph.D., for his friendship and for giving valuable suggestions to the manuscript. In addition, I want thank my roommate Anssi Lehikoinen, M.Sc. (tech.), for all the academic and non-academic discussions during these years.

I want to express my invaluable gratitude to my parents Tarja and Hannu and my brother Erno for their encouragement and support during my whole life. I also want thank all my friends, especially Timo, Timo and Aki, for friendship during these years.

Kuopio, January 7, 2008

Janne Huttunen

Abbreviations

1D	one-dimensional
2D	two-dimensional
EKF	extended Kalman filter
FE	finite element
FEM	finite element method
KF	Kalman filter
MR	magnetic resonance
PDE	partial differential equation
SMW	Sherman-Morrison-Woodbury (formula)
US	ultrasound

Notations

$\mathbb{R}$	the set of real numbers
$\mathbb{R}^n$	the n-dimensional Euclidean space
$\mathbb{X}$	the state space for the system state
$\mathbb{W}$	the state space for the state noise
$L^2(\mathbb{R})$	the Lebesgue space on $\mathbb{R}$
$H^2(\mathbb{R})$	the Sobolev space on $\mathbb{R}$
A^{T}	the adjoint operator of a linear operator A or the transpose of a matrix A
$\mathrm{Tr}\, A$	the trace of a matrix A
X_k	the state of the system
Y_k	the measurement vector
W_k	the state noise
V_k	the measurement noise
D_k	the measurements $(Y_1, \ldots, Y_k)$
d_k	a realization of D_k
X_k^r	the low–dimensional state
W_k^r	the state noise in the low–dimensional model
ϵ_k^r	the approximation error in the evolution model
ν_k^r	the approximation error in the observation model
$\widehat{X}_k$,$\widehat{X}_k^r$	the filter estimate for X_k and X_k^r (estimates based on $Y_1, \ldots, Y_k$)
$\widehat{\Gamma}_k$, $\widehat{\Gamma}_k^r$	the filter covariance estimate for X_k and X_k^r
$\widetilde{X}_k$, $\widetilde{X}_k^r$	the predictor for X_k and X_k^r (estimates based on $Y_1, \ldots, Y_{k-1}$)
$\widetilde{\Gamma}_k$, $\widetilde{\Gamma}_k^r$	the predictor covariance for X_k and X_k^r
N	the number of time instants
n	the dimension of the state in accurate model
m	the dimension of the measurement vector
r	the dimension of the low-dimensional state

LIST OF ORIGINAL PUBLICATIONS

This thesis consists of an overview and the following five original articles which are referred to in the text by their Roman numerals I-V:

I J.M.J. Huttunen and J.P. Kaipio. Approximation Errors In Nonstationary Inverse Problems. *Inverse Problems and Imaging*, 1:77-93, 2007.

II J.M.J. Huttunen and H.-K. Pikkarainen. Discretization error in dynamical inverse problems: one-dimensional model case. *Journal of Inverse And Ill-Posed Problems* 15:365-386, 2007.

III J.M.J. Huttunen and J.P. Kaipio. Approximation error analysis in nonlinear state estimation with an application to state-space identification. *Inverse Problems*, 23:2141-2157, 2007.

IV J.M.J. Huttunen, T. Huttunen, M. Malinen and J.P. Kaipio. Determination of heterogeneous thermal parameters using ultrasound induced heating and MR thermal mapping. *Physics in Medicine and Biology*, 51:1011–1032, 2006.

V J.M.J. Huttunen and J.P. Kaipio. Model reduction in state identification problems with an application to determination of distributed thermal parameters. *Applied Numerical Mathematics*, in review.

Contents

Chapter I

Introduction

Inverse problems are commonly understood as problems in which unobservable unknown quantities are inferred based on indirect observations from the unknown quantity. Inverse problems arise in several physical problems that are related, for example, to geophysics, astronomy and medical imaging. An example of inverse problems is the electrical impedance tomography (EIT) in which the electrical conductivity distribution ("image") inside the object is determined based on voltage measurements taken from the boundary of the object.

In this thesis we consider nonstationary inverse problems, i.e., the problems in which the unknown quantity is time-varying. Nonstationary inverse problems are most often treated as state estimation problems. State estimation problems can be seen as statistical inverse problems in which the time-varying unknown quantity is treated as the state of the system. The approach is Bayesian in that the prior model for the problem is comprised of the state evolution model with the aid of the model for the initial state. The evolution model together with the model describing the measurement process constitute the state space representation of the system.

Inverse problems are typically ill-posed problems in the sense that the problem has no unique solution and/or the solution depends discontinuously on the data. Therefore, inverse problems are very intolerant to both data errors and errors in associated models. In the statistical framework, this especially means that the uncertainties in the models have to be modelled properly.

There are typically two sources for the modelling errors. First, the physical model itself may include idealizations and other approximations which are not modelled properly in the model used in the computations. Second, several sources for the approximation errors are related to the construction of the computational model. For example, several nonstationary inverse problems are often induced by (stochastic) partial differential equations. In such cases some discretization scheme is typically employed to obtain a numerical form of the model. Another source for this type of errors is the truncation of the computational domain.

In this thesis we consider problems in which the errors are caused by the latter source. In such cases the required accuracy can be achieved with accurate numerical implementation. However, the accurate implementation often leads to very high dimensional models and the problems become computationally prohibitively complex for common state estimation schemes such as the Kalman filters. For example, in real-time applications,

such as in process tomography, the available time to compute the state estimate is of the order of milliseconds. This time is small when compared to the time which is required to compute the Kalman filter recursion using high-dimensional models. Therefore, approximative low-dimensional models have to be used in practical problems which, however, can compromise the accuracy of estimates.

The reduced accuracy of the models can be handled using the approximation error analysis. The approach is based on computing the approximative statistics of these errors. In this approach the high–dimensional model is used as a "supporting" model to which the solution obtained from the low–dimensional model is compared. The computation of the discrepancy between the models is carried out over the prior model of the state.

The stationary approximation error theory was proposed in [35, 36]. This approach has been applied successfully to several stationary problems including image reconstruction (deconvolution) [35, 36], electrical impedance tomography [35], optical tomography [5, 26] and geophysical tomography [44]. The infinite–dimensional nonstationary inverse problems related to stochastic PDEs have been treated in [56, 57]. In this approach the time–continuous problem is solved using the semigroup analysis and, in principle, the approach is applicable to such cases in which the associated semigroup is known or a computational semigroup representation can be formed.

There have also been other approaches to handle modelling and approximation errors. An approach in which modelling and approximation errors are represented using a stochastic driving term has been described in [20, 69]. However, this stochastic driving term is adjusted rather empirically in such a way that it is not based on the actual analysis of the errors. Discretization errors in so-called bounding problems have been considered in [41, 65]. These papers propose methods to compute the bounds for some linear functionals (e.g., to obtain confidence limits for the unknown quantity) so that discretization errors in associated model are taken into account. Discretization of unknown parameters in inverse problems is also considered in [42, 55, 43].

In this thesis we discuss generally the implementation of the approximation error approach for nonstationary inverse problems based on the approach presented in [35, 36]. The formulation used in this thesis allows us to handle both the errors due to the state reduction (using small dimensional approximation for the unknown) and increased time stepping in temporal integration. The approximation error methods are developed for both linear and nonlinear state estimation problems.

As applications, we consider four different problems. Two problems are related to the one dimensional heat equation. First, the temperature prediction in a one–dimensional rod is considered, and second, we estimate the thermal properties of this rod simultaneously with the temperature evolution using a state space approach. We also implement the numerical verification of the semigroup analysis presented in [56, 57]. As the last application we consider the determination of thermal parameters of tissue. In this measurement setting the distributed thermal conductivity and perfusion-related coefficient of tissue are determined by using ultrasound induced heating and magnetic resonance (MR) temperature imaging [51, 33].

Contents of this thesis

This thesis is organized as follows. In Chapter 2 approximation error models are derived for both linear and nonlinear state space representations. A brief review on the estimation of nonstationary parameters using state space approach is also given in this chapter. In Chapter 3 the Kalman filter recursions are extended for the approximation error

models. Furthermore, we present a computationally efficient form of the filter recursion for situations in which the number of measurements is high. In Chapter 4 we review the simulations carried out in the papers and summarize the results. Conclusions and discussion are given in Chapter 5.

CHAPTER II

State space models and model reduction

In this chapter we outline the approximation error approach used in this thesis. We construct an approximation error model which is the basis of the proposed approximation error methods. We also discuss a way to handle increased time stepping.

To make this presentation consistent with Publication III (in which a numerical verification for the semigroup analysis presented in [56, 57] is carried out), we consider the case in which the state spaces are general vector spaces. For example, these spaces can be, say, infinite–dimensional Banach or Hilbert spaces. Such situations occur often in physical systems in which the physical phenomenon is modelled with a partial differential equation (PDE) and the state of the system is a differentiable function or, more generally, an element in the Sobolev space.

However, if necessary, the state spaces can be interpreted as the Euclidean spaces $\mathbb{R}^n$ (in which case, for example, linear operators are simply matrices). Naturally, this will be the case in all practical computational problems. For example, if the system is modelled with a (stochastic) PDE, the solution of this equation is rarely known in closed form and therefore the infinite–dimensional model is typically unknown. Hence, some numerical discretization has to be employed.

For the theory of general vector spaces, the reader is referred, for example, to [59, 46, 28]. For stochastic analysis in $\mathbb{R}^n$, see [50, 73, 64, 40, 39], and in general vector spaces, see [58, 17].

2.1 State space models

In this thesis we consider only discrete-time state space models. This is warranted since, although the state of the system is often inherently continuous in time, measurements are nowadays typically obtained by sampling at discrete times. For continuous time state space models, see [38, 6, 50, 1].

Let $\mathbb{X}$ and $\mathbb{W}$ be measurable vector spaces. Assume that an $\mathbb{X}$-valued stochastic process $\{X_k\}_{k=0}^N$ representing the state of the system satisfies the state space model

$$\begin{cases} X_{k+1} = F_{k+1}(X_k, W_{k+1}), & k = 0, \ldots, N-1, \\ Y_k = G_k(X_k) + V_k, & k = 1, \ldots, N, \end{cases} \tag{2.1}$$

where $\{W_k\}_{k=1}^N$ is a $\mathbb{W}$-valued stochastic process representing the state noise, $\{Y_k\}_{k=1}^N$ and $\{V_k\}_{k=1}^N$ are $\mathbb{R}^m$-valued stochastic processes representing measurements and measurement

noise, respectively, and F_k and G_k are measurable mappings (if the spaces $\mathbb{X}$ and $\mathbb{W}$ are topological vector spaces, such as $\mathbb{R}^n$, a sufficient condition for measurability is, say, continuity). The former equation describes temporal behavior of the system and is often called as the *evolution model*. The latter equation provides interdependence between the state and the measurement and is called the *observation model*. Due to the practical reasons we assume that Y_k and V_k are finite–dimensional elements. Furthermore, in this thesis we treat only the additive error model for the observations. However, the generalization to nonadditive models is straightforward.

The state space model (2.1) is assumed to be adequately accurate in the sense that the modelling errors are negligible with respect to the magnitude of the state and observation noise processes. Often the model (2.1) is not suitable for state space estimation due to computational reasons. First of all, if the state space is infinite-dimensional, the state cannot be represented using finite number of freedoms. Hence, we have to discretize the state space model (2.1), i.e., approximate the state in a finite dimensional subspace. Moreover, in the case of a finite–dimensional state space $\mathbb{X} = \mathbb{R}^n$, accurate modelling of a physical phenomenon often leads to a situation in which the dimension of the model n is required to be very large and the model becomes computationally excessively complex.

To overcome this problem, we approximate the state in a relatively low dimensional subspace of dimension r. We identify elements in this subspace with coordinates in some given basis so that the subspace can be treated as the Euclidean space $\mathbb{R}^r$. Let $\{X_k^r\}_{k=0}^N$ be an $\mathbb{R}^r$-valued stochastic process satisfying the approximate low–dimensional model

$$\begin{cases} X_{k+1}^r = F_{k+1}^r(X_k^r, W_{k+1}^r), & k = 0, \ldots, N-1, \\ Y_k = G_k^r(X_k^r) + V_k, & k = 1, \ldots, N, \end{cases} \tag{2.2}$$

where F_k^r and G_k^r are known measurable mappings and $\{W_k^r\}_{k=1}^N$ is an $\mathbb{R}^s$-valued process representing state noise. This model can be constructed using model reduction techniques or in PDE induced problems using sparse meshes in the numerical discretization. For model reduction techniques for linear problems, see [4].

The use of the approximative model (2.2) can lead to large modelling errors which compromise the estimation accuracy. In Section 2.2 we analyze this modelling error and construct a so-called enhanced error model in which the modelling errors are taken into account.

In the sequel, we call the state X_k^r as the *reduced state* and the state space model (2.2) as the *reduced model*. Furthermore, the state X_k is referred as the *accurate state* and the model (2.1) as the *accurate model*.

2.2 Construction of the enhanced error model

Assume that the reduced state is given by a linear mapping $P_r : \mathbb{X} \to \mathbb{R}^r$ such that $X_k^r = P_r X_k$. Furthermore, we assume that $W_k^r = P_{\mathrm{w}} W_k$ for some linear operator P_{w}. The mapping P_r is typically a projection or, in a PDE induced problems, P_r can chosen to be an interpolation mapping between the computational meshes that are used in the construction of the accurate and reduced models. The choice of the operator P_{w} depends on the form of the reduced and accurate models. In some situations we can choose $P_{\mathrm{w}} = 0$ which corresponds to the case when the reduced model is treated as a deterministic model in which the term W_k^r does not appear.

The core of the approach is as follows. We can write

$$\begin{aligned} X_{k+1}^r &= P_r F_{k+1}(X_k, W_{k+1}) \\ &= F_{k+1}^r(X_k^r, W_{k+1}^r) \\ &\quad + P_r F_{k+1}(X_k, W_{k+1}) - F_{k+1}^r(P_r X_k, P_{\mathrm{w}} W_{k+1}) \\ &= F_{k+1}^r(X_k^r, W_{k+1}^r) + \epsilon_{k+1}^r \end{aligned} \tag{2.3}$$

for all $k = 0, \ldots, N-1$, where the stochastic process

$$\epsilon_k^r := P_r F_k(X_{k-1}, W_k) - F_k^r(P_r X_{k-1}, P_{\mathrm{w}} W_k), \quad k = 1, \ldots, N, \tag{2.4}$$

represents the approximation error in the evolution equation. Similarly, for the observation model we have

$$\begin{aligned} Y_k &= G_k(X_k) + V_k \\ &= G_k^r(X_k^r) + G_k(X_k) - G_k^r(P_r X_k) + V_k \\ &= G_k^r(X_k^r) + \nu_k^r + V_k \end{aligned} \tag{2.5}$$

for all $k = 1, \ldots, N$, where the stochastic process

$$\nu_k^r := G_k(X_k) - G_k^r(P_r X_k), \quad k = 1, \ldots, N, \tag{2.6}$$

represents the approximation error in the observation equation.

Equations (2.3) and (2.5) form a low–dimensional state model for the problem:

$$\begin{cases} X_{k+1}^r = F_{k+1}^r(X_k^r, W_{k+1}^r) + \epsilon_{k+1}^r, & k = 0, \ldots, N-1 \\ Y_k = G_k^r(X_k^r) + \nu_k^r + V_k, & k = 1, \ldots, N. \end{cases} \tag{2.7}$$

The statistics of the model (2.7) conforms to the accurate model (2.1) when the statistics of the approximation error processes $\{\epsilon_k^r\}$ and $\{\nu_k^r\}$ are known. In the sequel, the model (2.7) is called as the *enhanced error model*. This term is also used in [35, 36], although in these references this term refers to the model in which interdependence of the approximation error and the unknown quantity, the state in our case, is ignored.

Our major goal is to use the enhanced error model (2.7) in the solution of the state space estimation problem. The Kalman filter (KF) recursions [37] in their usual form are not directly applicable with the enhanced error model (2.7) due to the fact that the error processes ϵ_k^r and ν_k^r depend on the state. Hence, to use the enhanced error model (2.7), we need to extend the KF recursions for the state dependent error terms. This extension is presented in Chapter 3.

It is to be noted that the use of the accurate model cannot be avoided completely, since this model has to be used in the determination of the statistics of the approximation error terms. However, our purpose is to avoid its use in the filtering recursion such that all calculations in which this model has to be used can be completed before any measurements are taken and need to be carried out only once for each measurement setting.

Enhanced error model in the linear case

In the linear case we can use slightly different but a more straightforward approach. The difference between these approaches is only formal and is related to the way how the state noise is treated.

The accurate linear state model studied in this thesis is of the form

$$\begin{cases} X_{k+1} = A_{k+1}X_k + B_{k+1}U_{k+1} + W_{k+1}, & k = 0, \dots, N-1, \\ Y_k = C_k X_k + D_k \widetilde{U}_k + V_k, & k = 1, \dots, N, \end{cases} \tag{2.8}$$

where $\{U_k\}_{k=1}^N$ and $\{\widetilde{U}_k\}_{k=1}^N$ are stochastic processes representing input or possibly control and A_k, B_k, C_k and D_k are measurable linear operators. The related reduced model is of the form

$$\begin{cases} X^r_{k+1} = A^r_{k+1}X^r_k + B^r_{k+1}U_{k+1} + \bar{W}^r_{k+1}, & k = 0, \dots, N-1, \\ Y_k = C^r_k X^r_k + D^r_k \widetilde{U}_k + \bar{V}_k, & k = 1, \dots, N, \end{cases} \tag{2.9}$$

where A^r_k, B^r_k, C^r_k and D^r_k are matrices and $\{\bar{W}^r_k\}_{k=1}^N$ and $\{\bar{V}_k\}_{k=1}^N$ are noise processes. The key realization in the approach is that the processes $\bar{W}^r_k$ and $\bar{V}_k$ are not directly given by the processes W_k and V_k. Our main purpose in this approach is to determine the processes $\bar{W}_k$ and $\bar{V}_k$.

Again, due to the the interdependency $X^r_k = P_r X_k$, we can write

$$\begin{aligned} X^r_{k+1} &= P_r(A_{k+1}X_k + B_{k+1}U_{k+1} + W_{k+1}) \\ &= A^r_{k+1}X^r_k + B^r_{k+1}U_{k+1} + (P_r A_{k+1} - A^r_{k+1}P_r)X_k \\ &\quad + (P_r B_{k+1} - B^r_{k+1})U_{k+1} + P_r W_{k+1} \\ &= A^r_{k+1}X^r_k + B^r_{k+1}U_{k+1} + \epsilon^r_{k+1} + W^r_{k+1} \end{aligned} \tag{2.10}$$

for all $k = 0, \dots, N-1$, where the processes $\{\epsilon^r_k\}_{k=1}^N$ and $\{W^r_k\}_{k=1}^N$ are given by

$$\epsilon^r_k := (P_r A_k - A^r_k P_r)X_{k-1} + (P_r B_k - B^r_k)U_k \quad \text{and} \quad W^r_k := P_r W_k$$

for all $k = 1, \dots, N$. Furthermore, the observation model can be written as

$$\begin{aligned} Y_k &= C_k X_k + D_k \widetilde{U}_k + V_k \\ &= C^r_k X^r_k + D^r_k \widetilde{U}_k + (C_k - C^r_k P_r)X_k + (D_k - D^r_k)\widetilde{U}_k + V_k \\ &= C^r_k X^r_k + D^r_k \widetilde{U}_k + \nu^r_k + V_k \end{aligned} \tag{2.11}$$

for all $k = 1, \dots, N$, where the process $\{\nu^r_k\}_{k=1}^N$ is given by

$$\nu^r_k := (C_k - C^r_k P_r)X_k + (D_k - D^r_k)\widetilde{U}_k, \quad k = 1, \dots, N.$$

Equations (2.10) and (2.11) form the linear enhanced error model. Note that in this case the approximation error term ϵ^r_k does not depend on the state noise.

2.3 Temporal discretization

Most often the evolution models are induced by (stochastic) differential equations or PDEs. In such cases the time step in temporal integration is usually required to be smaller than the physical time between two measurements. For instance, if the physical model for evolution is a parabolic PDE, the spatially discretized form is a stiff differential equation which calls for a very dense temporal discretization, especially in the case of the accurate model. In this section, the aim is to use small time stepping in the evolution model.

It is to be noted that approximation errors due to temporal integration are implicitly handled when this approach is used. Namely, while the time stepping for the reduced

model is chosen to be rather long so that the model is sufficient for estimation, the time stepping for the accurate evolution model can be chosen to be very short so that errors caused by temporal integration are negligible.

The evolution model corresponding to small time stepping is written as

$$\bar{X}_{j+1} = \bar{F}_{j+1}(\bar{X}_j, \bar{W}_{j+1}), \quad j = 0, \ldots, \bar{N} - 1, \tag{2.12}$$

where $\bar{X}_j$ is the state of the system, $\bar{W}_j$ is the state noise and $\bar{F}_j$ are known mappings. We assume that the values of $\bar{X}_k$ are in $\mathbb{X}$, the values of $\bar{W}_j$ are in a measurable vector space $\bar{\mathbb{W}}$ and the mappings $\bar{F}_j$ are measurable. We form a mapping F_k and a process W_k for an evolution model corresponding to measurement times.

For simplicity, the time between measurements is assumed to be a multiple of the time step in temporal integration, that is, $X_k = \bar{X}_{kN_d}$ for some integer N_d. We use Eq. (2.12) to compute X_{k+1} from X_k recursively, i.e., we start from X_k and update state N_d times by using Equation (2.12). Hence, F_{k+1} is chosen to be a mapping $(x, w) \mapsto y$ where $w = (w_1, \ldots, w_{N_d})$ and y is given by the iterative equations

$$\begin{aligned} &x_0 = x, \\ &x_{j+1} = \bar{F}_{kN_d+j+1}(x_j, w_{j+1}), \quad j = 0, \ldots, N_d - 1, \\ &y = x_{N_d}. \end{aligned}$$

Then $X_{k+1} = F_{k+1}(X_k, W_{k+1})$ where the state noise is chosen to be $W_{k+1} = (\bar{W}_{kN_d+1}, \ldots, \bar{W}_{kN_d+N_d})$ and $\mathbb{W} = \bar{\mathbb{W}}^{N_d}$.

2.4 Nonstationary parameter estimation problems

In practical problems one or more terms in the state space model are often at least partially unknown. For example, the state noise covariance in the evolution equation is not usually well known. Furthermore, if the state space model is induced by, say, thermal equation, the thermal conductivity may be an unknown constant or even a distributed parameter. In this section we consider the estimation of such parameters.

Consider the following nonlinear state space model

$$\begin{cases} X_{k+1} = F_{k+1}(X_k, \theta, W_{k+1}), & k = 0, \ldots, N-1, \\ Y_k = G_k(X_k, \theta) + V_k, & k = 1, \ldots, N, \end{cases}$$

where θ_k are unknown parameters. The problem is to estimate θ based on measurements $Y_1, \ldots, Y_N$. There are several techniques which can be used to estimate unknown parameters in state space models. For example, if the unknown parameters are time-invariant, we can try to construct the likelihood function $\ell(Y_1, \ldots, Y_N|\theta)$ and determine the maximum likelihood estimate for θ. This kind of approach is used in Publication IV to estimate thermal conductivity and perfusion related coefficient in biological thermal equation, the Pennes' bioheat equation [53]. For other techniques, see [2, Chapter 10] and [24, Section 7.3]. In this section we use an adaptive estimation approach in which the state vector is augmented to include the unknown parameter to form a state space model of the form (2.1).

We treat the unknown parameters θ as a stochastic process $\{\theta_k\}_{k=0}^N$ and set $X_k^{\mathrm{A}} = (X_k, \theta_k)$. We employ a random walk model for the unknown parameters,

$$\theta_{k+1} = \theta_k + \omega_{k+1}, \quad k = 0, \ldots, N-1,$$

where $\{\omega_k\}_{k=1}^N$ is a state noise process. If θ_k is assumed to be stationary, we can set $\theta_{k+1} = \theta_k$, i.e., choose $\omega_k = 0$. Furthermore, more complicated models can also be straightforwardly used. Note that if $\omega_k = 0$, the distribution of θ_k is determined by the distribution of the initial state.

The evolution model for X_k^{A} is given by

$$X_{k+1}^{\mathrm{A}} = \begin{pmatrix} X_{k+1} \\ \theta_{k+1} \end{pmatrix} = \begin{pmatrix} F_{k+1}(X_k, \theta_k, W_{k+1}) \\ \theta_k + \omega_{k+1} \end{pmatrix} =: F_{k+1}^{\mathrm{A}}(X_k^{\mathrm{A}}, W_{k+1}^{\mathrm{A}}), \tag{2.13}$$

where $W_k^{\mathrm{A}} = (W_k, \omega_k)$. The estimates for the augmented state X_k^{A} can be computed by using standard state estimation techniques. Approximation errors can be taken into account by applying the approach described in Section 2.2 to model (2.13). For details, see Publication V.

CHAPTER III

State estimation

Kalman filter (KF) methods [37] are commonly used for state estimation problems. However, the error terms in the enhanced error model are not independent of the state and therefore KF in its usual form is not applicable. In this chapter we present an extension for KF to accommodate the linear enhanced error model. Furthermore, we derive equations for nonlinear state space estimator, that is, the extended Kalman filter (EKF). Finally, we present a modification to the presented extension for a case in which the number of measurements is high. For general texts on Kalman filtering, see [2, 18, 10, 7, 25]. For nonstationary inverse problems that are cast in the state space formalism, see [34, 35, 63].

Throughout this chapter the following notations are used. For $k = 1, \ldots, N$, we denote the measurements by $\mathrm{D}_k := (Y_1, \ldots, Y_k)$ and realizations of D_k by $d_k = (y_1, \ldots, y_k)$. If X and Y are random variables, the conditional expectation and covariance of X given a realization $\mathrm{D}_k = d_k$ are denoted by $\mathbb{E}^{d_k}[X]$ and $\mathrm{cov}^{d_k}(X)$, respectively, and the cross-covariance of X and Y given $\mathrm{D}_k = d_k$ is denoted by $\mathrm{cov}^{d_k}(X, Y)$. If the state space is the Euclidean space $\mathbb{R}^n$, the conditional covariance and the conditional cross-covariance are matrices whose components are

$$(\mathrm{cov}^{d_k}(X))_{ij} = \mathbb{E}^{d_k}\left[((X)_i - \mathbb{E}^{d_k}[(X)_i])((X)_j - \mathbb{E}^{d_k}[(X)_j])\right],$$
$$(\mathrm{cov}^{d_k}(X, Y))_{ij} = \mathbb{E}^{d_k}\left[((X)_i - \mathbb{E}^{d_k}[(X)_i])((Y)_j - \mathbb{E}^{d_k}[(Y)_j])\right],$$

where $(X)_i$ is the ith component of X. For the definition in infinite–dimension spaces, see [58]. If $k = 0$, notations $\mathbb{E}^{d_0}[X]$, $\mathrm{cov}^{d_0}(X)$ and $\mathrm{cov}^{d_0}(X, Y)$ refer to the conventional expectation, covariance and cross-covariance.

3.1 State estimation and Kalman filtering

In this section we give a brief review on state estimation and derive equations for the Kalman filter recursion. We concentrate on estimating the state X_k which satisfies the linear state space model (2.8), or

$$X_{k+1} = A_{k+1}X_k + B_{k+1}U_{k+1} + W_{k+1}, \qquad k = 0, \ldots, N-1, \tag{3.1}$$
$$Y_k = C_kX_k + D_k\widetilde{U}_k + V_k, \qquad k = 1, \ldots, N. \tag{3.2}$$

To completely specify the statistics of the state, we need to specify the distributions of the initial state X_0 and the processes U_k, $\widetilde{U}_k$, W_k and V_k. In this section, we assume that the state spaces $\mathbb{X}$ and $\mathbb{W}$ are Euclidean spaces.

The aim is to estimate the state X_k based on measurements $Y_1, \ldots, Y_k$. From the statistical point of view, the degree of information concerning the state X_k provided by these measurements is coded in the conditional distribution of X_k given $\mathrm{D}_k = d_k$, denoted by $\widehat{\mu}_k$. Hence the overall problem is to determine $\widehat{\mu}_k$ for all $k = 1, \ldots, N$. This problem is called the *filtering problem.*

We consider here only the case in which the associated processes and distributions are Gaussian. Since Gaussian distributions are completely determined by the mean and covariance of the distribution, it is sufficient to determine the mean and covariance of $\widehat{\mu}_k$, which are denoted by $\widehat{X}_k$ and $\widehat{\Gamma}_k$, respectively.

The mean $\widehat{X}_k$ can be treated as a point estimate of X_k. Furthermore, the covariance $\widehat{\Gamma}_k$ can be treated as the covariance of estimation error. In the sequel, these quantities are called as the *filter estimate* and *filter covariance.* It is to be noted that $\widehat{X}_k$ and $\widehat{\Gamma}_k$ are the conditional expectation and covariance of X_k given $\mathrm{D}_k = d_k$ and this conditional expectation is, even without the assumptions about Gaussianity, an optimal estimator for X_k based on data D_k in the sense that it minimizes the variance of estimation error, see for example [50, Chapter 6].

We assume that the processes in the state space model (3.1)–(3.2) satisfy the following assumptions::

(i) the initial state X_0 and the noise processes $\{W_k\}$ and $\{V_k\}$ are Gaussian;

(ii) U_k and $\widetilde{U}_k$ are general Gaussian random variables for all $k = 1, \ldots, N$;

(iii) X_0 is independent of $U_k, \widetilde{U}_k, W_k$, and V_k for all $k = 1, \ldots, N$;

(iv) U_{k+1}, W_{k+1}, $\widetilde{U}_k$, and V_k are independent for every $k = 1, \ldots, N-1$, and U_1 and W_1 are independent;

(v) for every $k, \ell = 1, \ldots, N$ such that $k \neq \ell$, (U_k, W_k) and (U_ℓ, W_ℓ) are independent, as well as $(\widetilde{U}_k, V_k)$ and $(\widetilde{U}_\ell, V_\ell)$;

(vi) the expectations of W_k and V_k are zero for all $k = 1, \ldots, N$.

The assumption (ii) for U_k and $\widetilde{U}_k$ means that the characteristic functions of these random variables are of the form $\phi(u) = \exp\left(\mathrm{i}m^{\mathrm{T}}u - 1/2u^{\mathrm{T}}Cu\right)$ for a vector m and a symmetric non-negative definite matrix C [50, Appendix A]. For example, U_k and $\widetilde{U}_k$ can be deterministic processes or control inputs computed based on the state estimates. It is to be noted that the above conditions are not rigorous. For example, correlated noise vectors has been treated in [2]. Furthermore, the assumption (vi) is made only to simplify notations and it is trivial to take into account nonzero expectations.

By the above assumptions, the random variables X_k and $Y_1, \ldots, Y_k$ are jointly Gaussian for all $k = 1, \ldots, N$ (see Publication I). Hence $\widehat{\mu}_k$ is Gaussian and its expectation and covariance are given by the formulas

$$\begin{aligned} \widehat{X}_k &= \mathbb{E}[X_k] + \mathrm{cov}(X_k, \mathrm{D}_k)\mathrm{cov}(\mathrm{D}_k)^{-1}(d_k - \mathbb{E}[Y_k]), \\ \widehat{\Gamma}_k &= \mathrm{cov}(X_k) - \mathrm{cov}(X_k, \mathrm{D}_k)\mathrm{cov}(\mathrm{D}_k)^{-1}\mathrm{cov}(\mathrm{D}_k, X_k), \end{aligned}$$

see for example [35, Theorem 3.5]. However, since the dimension of D_k increases over time, these equations are often inappropriate for practical situations.

The Kalman filtering methods are recursive. The aim is to determine $\widehat{\mu}_{k+1}$ from $\widehat{\mu}_k$ based on the evolution model as well as the information provided by the measurement

$Y_{k+1} = y_{k+1}$. This task is divided into two separate problems: the *time update* problem is to determine the conditional distribution of X_{k+1} given D_k, denoted by $\widetilde{\mu}_k$, and the *observation update* problem is to use information provided by Y_{k+1} to determine $\widehat{\mu}_{k+1}$. We denote the mean and covariance of $\widetilde{\mu}_{k+1}$ by $\widetilde{X}_{k+1}$ and $\widetilde{\Gamma}_{k+1}$. From the statistical point of view, $\widetilde{X}_{k+1}$ is the best estimate for X_{k+1} based on data $\mathrm{D}_k = d_k$. In the sequel $\widetilde{X}_{k+1}$ and $\widetilde{\Gamma}_{k+1}$ are referred to as the *predictor* and the *predictor covariance*.

The solution for the time update problem can be calculated using the evolution model (3.1) and the above independence assumptions. The predictor and predictor covariance are given by the equations

$$\widetilde{X}_{k+1} = A_{k+1}\widehat{X}_k + B_{k+1}\eta^u_{k+1}, \tag{3.3}$$

$$\widetilde{\Gamma}_{k+1} = A_{k+1}\widehat{\Gamma}_k A^{\mathrm{T}}_{k+1} + B_{k+1}\Sigma^u_{k+1}B^{\mathrm{T}}_{k+1} + \Sigma^w_{k+1}, \tag{3.4}$$

where η^u_{k+1} and Σ^u_{k+1} are the expectation and covariance of U_{k+1}, and Σ^w_{k+1} is the covariance of W_{k+1}. For details, see Publication I.

The solution for the observation update problem is given by the equations

$$\widehat{X}_{k+1} = \widetilde{X}_{k+1} + \mathrm{cov}^{d_k}(X_{k+1}, Y_{k+1})\mathrm{cov}^{d_k}(Y_{k+1})^{-1}(y_{k+1} - \mathbb{E}^{d_k}[Y_{k+1}]), \tag{3.5}$$

$$\widehat{\Gamma}_{k+1} = \widetilde{\Gamma}_{k+1} - \mathrm{cov}^{d_k}(X_{k+1}, Y_{k+1})\mathrm{cov}^{d_k}(Y_{k+1})^{-1}\mathrm{cov}^{d_k}(Y_{k+1}, X_{k+1}), \tag{3.6}$$

see for example Publication I. The conditional expectation and covariance of Y_{k+1} given $\mathrm{D}_k = d_k$ as well as the conditional cross-covariance of X_{k+1} and Y_{k+1} given $\mathrm{D}_k = d_k$ can be computed using the observation model (3.2) and the independence assumptions as shown in Publication I. As the result, we get the following equations

$$\widehat{X}_{k+1} = \widetilde{X}_{k+1} + K_{k+1}(y_{k+1} - C_{k+1}\widetilde{X}_{k+1} - D_{k+1}\eta^{\widetilde{u}}_k), \tag{3.7}$$

$$\widehat{\Gamma}_{k+1} = (I - K_{k+1}C_{k+1})\widetilde{\Gamma}_{k+1}, \tag{3.8}$$

$$K_{k+1} := \widetilde{\Gamma}_{k+1}C^{\mathrm{T}}_{k+1}(C_{k+1}\widetilde{\Gamma}_{k+1}C^{\mathrm{T}}_{k+1} + D_{k+1}\Sigma^{\widetilde{u}}_{k+1}D^{\mathrm{T}}_{k+1} + \Sigma^v_{k+1}), \tag{3.9}$$

where $\eta^{\widetilde{u}}_{k+1}$ and $\Sigma^{\widetilde{u}}_{k+1}$ are the expectation and covariance of $\widetilde{U}_{k+1}$, respectively, and Σ^v_{k+1} is the covariance of V_{k+1}. Equations (3.3), (3.4) and (3.7)–(3.9) form an estimator which is known as the Kalman filter. The matrix K_{k+1} is commonly called the *Kalman gain matrix*.

There are various forms for the KF recursion equations. The form of the filter presented above is usually known as the *innovation filter*. In other forms, the equations are expressed, for example, in terms of the inverses of the covariances $\widehat{\Gamma}_k$ and $\widetilde{\Gamma}_k$ (*information filter*) or the matrix square roots of these covariances (*square root filters*), see for example [2, 21]. In the following we present the information filter form.

Information filter

The innovation filter form of Kalman filter equations is computationally efficient in problems in which the dimension of the state vector is greater than the number of measurements. However, in several practical problems the situation is reversed. The information filter form of the Kalman filter recursion is computationally more efficient for cases in which the dimension of the measurement vector is high.

The information filter is based on the Sherman-Morrison-Woodbury (SMW) formula (also known as the matrix inversion lemma) [29, 23]

$$(QRQ^{\mathrm{T}} + P)^{-1} = P^{-1} - P^{-1}Q(Q^{\mathrm{T}}P^{-1}Q + R^{-1})^{-1}Q^{\mathrm{T}}P^{-1},$$

where P, R and Q are appropriate size matrices such that R and P are invertible. The basic idea is to apply the SMW equation to the Kalman filter recursion to yield new filtering equations for a filter which is expressed in terms of the inverses of $\widehat{\Gamma}_k$ and $\widetilde{\Gamma}_k$. These matrices are called as *information matrices*.

We assume that the matrix A_k is invertible. Furthermore, for simplicity, we assume that the state space model does not contain input terms U_k and $\widetilde{U}_k$. The information filter equations are written in terms of the variables $\widehat{a}_k = \widehat{\Gamma}_k^{-1}\widehat{X}_k$ and $\widetilde{a}_k = \widetilde{\Gamma}_k^{-1}\widetilde{X}_k$, which can be updated recursively by the using the equations [2]

$$\begin{aligned}
\widetilde{a}_{k+1} &= (I - L_{k+1})A_{k+1}^{-1}\widehat{a}_k \\
\widetilde{\Gamma}_{k+1}^{-1} &= (I - L_{k+1})A_{k+1}^{-1\ \mathrm{T}}\widehat{\Gamma}_k^{-1}A_{k+1}^{-1} \\
\widehat{a}_{k+1} &= \widetilde{a}_{k+1} + C_{k+1}^{\mathrm{T}}\Sigma_{k+1}^{v}y_{k+1} \\
\widehat{\Gamma}_{k+1}^{-1} &= \widetilde{\Gamma}_{k+1}^{-1} + C_{k+1}^{\mathrm{T}}\Sigma_{k+1}^{v\ -1}C_{k+1}
\end{aligned}$$

where the matrix L_{k+1} is

$$L_{k+1} = A_{k+1}^{\mathrm{T}\ -1}\widehat{\Gamma}_k^{-1}A_{k+1}^{\mathrm{T}\ -1}(A_{k+1}^{-1\ \mathrm{T}}\widehat{\Gamma}_k^{-1}A_{k+1}^{-1} + \Sigma_{k+1}^{w\ -1})^{-1}.$$

The above equations form the information filter. The filter estimate and the predictor can be recovered by solving the algebraic equations $\widetilde{X}_k = \widetilde{\Gamma}_k\widetilde{a}_k$ and $\widehat{X}_k = \widehat{\Gamma}_k\widehat{a}_k$ when $\widetilde{\Gamma}_k^{-1}$ and $\widehat{\Gamma}_k^{-1}$ are known.

3.2 Extension for the enhanced error model

In this section we derive an estimator for X_k^r based on the enhanced error model (2.11), or

$$X_{k+1}^r = A_{k+1}^r X_k^r + B_{k+1}^r U_{k+1} + \epsilon_{k+1}^r + W_k^r, \qquad k = 0, \ldots, N-1 \tag{3.10}$$

$$Y_k = C_k^r X_k^r + D_k^r \widetilde{U}_k + \nu_k^r + V_k, \qquad k = 1, \ldots, N. \tag{3.11}$$

The filter estimate and the filter covariance for X_k^r are denoted by $\widehat{X}_k^r$ and $\widehat{\Gamma}_k^r$, respectively. Furthermore, the predictor and the predictor covariance for X_k^r are denoted by $\widetilde{X}_k^r$ and $\widetilde{\Gamma}_k^r$, respectively.

We assume that the state spaces $\mathbb{X}$ and $\mathbb{W}$ are real separable Hilbert spaces. To ensure Gaussianity, we assume that the assumptions in Section 3.1 for the accurate model (3.1)–(3.2) are satisfied. In addition, we need also to assume that the linear operators A_k, B_k, C_k and D_k are bounded for all $k = 1, \ldots, N$. Then, for all $k = 1, \ldots, N$, the joint distribution of X_k and $Y_1, \ldots, Y_k$ is Gaussian and, since X_k^r is a linear image of X_k, the joint distribution of X_k^r and $Y_1, \ldots, Y_k$ is also jointly Gaussian.

The solutions for the time and observation update problems are obtained similarly as in Section 3.1. The evolution model (3.10) gives

$$\widetilde{X}_{k+1}^r = A_{k+1}^r \widehat{X}_k^r + B_{k+1}^r \eta_{k+1}^u + \mathbb{E}^{d_k}\left[\epsilon_{k+1}^r\right], \tag{3.12}$$

$$\begin{aligned}
\widetilde{\Gamma}_{k+1}^r = {} & A_{k+1}^r \widehat{\Gamma}_k^r A_{k+1}^{r\ \mathrm{T}} + B_{k+1}^r \Sigma_{k+1}^u B_{k+1}^{r\ \mathrm{T}} + \mathrm{cov}^{d_k}(\epsilon_{k+1}^r) + \Sigma_{k+1}^{w,r} \\
& + A_{k+1}^r \mathrm{cov}^{d_k}(X_k^r, \epsilon_{k+1}^r) + \mathrm{cov}^{d_k}(\epsilon_{k+1}^r, X_k^r) A_{k+1}^{r\ \mathrm{T}} \\
& + B_{k+1}^r \mathrm{cov}^{d_k}(U_{k+1}, \epsilon_{k+1}^r) + \mathrm{cov}^{d_k}(\epsilon_{k+1}^r, U_{k+1}) B_{k+1}^{r\ \mathrm{T}},
\end{aligned} \tag{3.13}$$

where $\Sigma^{w,r}_{k+1}$ is the covariance of W^r_{k+1}, that is, $\Sigma^{w,r}_{k+1} = P_r \Sigma^w_{k+1} P_r^{\mathrm{T}}$. Substitution of the observation model (3.11) to Equations (3.5)–(3.6) gives

$$\begin{aligned}
\widehat{X}^r_{k+1} &= \widetilde{X}^r_{k+1} + K^r_{k+1}(y_{k+1} - C^r_{k+1}\widetilde{X}^r_{k+1} - D^r_{k+1}\eta^{\widetilde{u}}_k - \mathbb{E}^{d_k}[\nu^r_{k+1}]), && (3.14)\\
\widehat{\Gamma}^r_{k+1} &= \widetilde{\Gamma}^r_{k+1} - K^r_{k+1}(C^r_{k+1}\widetilde{\Gamma}^r_{k+1} + \mathrm{cov}^{d_k}(\nu^r_{k+1}, X^r_{k+1})), && (3.15)\\
K^r_{k+1} &:= (\widetilde{\Gamma}^r_{k+1} C^{r\,\mathrm{T}}_{k+1} + \mathrm{cov}^{d_k}(X^r_{k+1}, \nu^r_{k+1}))\\
&\quad \times \{C^r_{k+1}\widetilde{\Gamma}^r_{k+1} C^{r\,\mathrm{T}}_{k+1} + D^r_{k+1}\Sigma^{\widetilde{u}}_{k+1} D^{r\,\mathrm{T}}_{k+1} + \mathrm{cov}^{d_k}(\nu^r_{k+1}) + \Sigma^v_{k+1}\\
&\quad + C^r_{k+1}\mathrm{cov}^{d_k}(X^r_{k+1}, \nu^r_{k+1}) + \mathrm{cov}^{d_k}(\nu^r_{k+1}, X^r_{k+1}) C^{r\,\mathrm{T}}_{k+1}\\
&\quad + D^r_{k+1}\mathrm{cov}^{d_k}(\widetilde{U}_{k+1}, \nu^r_{k+1}) + \mathrm{cov}^{d_k}(\nu^r_{k+1}, \widetilde{U}_{k+1}) D^{r\,\mathrm{T}}_{k+1}\}^{-1}. && (3.16)
\end{aligned}$$

Equations (3.12)–(3.16) can be used as an estimator for X^r_k if the conditional expectations, covariances and cross-covariances related to ϵ^r_{k+1} and ν^r_{k+1} are determined. The computation of these terms are described in Section 3.4. For the initial state we have $\widehat{X}^r_0 = \mathbb{E}[X^r_0] = P_r \mathbb{E}[X_0]$ and $\widehat{\Gamma}^r_0 = \mathrm{cov}(X^r_0) = P_r \mathrm{cov}(X_0) P_r^{\mathrm{T}}$.

3.3 Extension to nonlinear filtering problems

In this section we derive filtering equations for the nonlinear enhanced error model (2.7). A similar approach is typically used to extend the KF recursion for nonlinear state space models (the extended Kalman filter, EKF), see for example [2].

There are different approaches to handle nonlinear state-space models. First of all, we can linearize the state space model around some fixed point and use this linearized model with the linear KF recursion formulas. This leads to a very simple method which, however, works only with slightly nonlinear models. An another approach is to linearize the state space model at each iteration step around the current state estimate. This approach is the most commonly used and therefore we follow it in this thesis. There is also an approach known as the iterated extended Kalman filter (IEKF), in which the observation update problem is solved iteratively.

It is to be noted that, due to the linearizations and other approximations, the resulting estimates and error covariances are mere approximations for the corresponding conditional expectations and covariances. The exact conditional expectation and covariance as well as the complete statistical structure can only be obtained with the excessively heavy Markov chain Monte Carlo type schemes such as particle filters [72, 15].

As in the previous section, the filter estimate and filter covariance are denoted by $\widehat{X}^r_k$ and $\widehat{\Gamma}^r_k$, respectively, and the predictor and predictor covariance are denoted by $\widetilde{X}^r_k$ and $\widetilde{\Gamma}^r_k$, respectively. However, although in the previous section $\widehat{X}^r_k$ and $\widehat{\Gamma}^r_k$ were the conditional expectation and covariance of X^r_k given $\mathrm{D}_k = d_k$, referring to the above, in this section $\widehat{X}^r_k$ and $\widehat{\Gamma}^r_k$ are only approximations for these quantities. Same applies to $\widetilde{X}^r_k$ and $\widetilde{\Gamma}^r_k$.

Assume that F^r_k and G^r_k are differentiable for all $k = 1, \ldots, N$. Then Taylor's formula gives an approximation for the evolution model

$$X^r_{k+1} \approx F^r_{k+1}(x^*, 0) + \partial_x F^r_{k+1}(X^r_k - x^*) + \partial_w F_{k+1} W^r_k + \epsilon^r_k$$

where x^* is a linearization point and $\partial_x F^r_{k+1}$ and $\partial_w F^r_{k+1}$ are the Jacobian matrices of F^r_{k+1} with respect to x and w, respectively, evaluated at the point $(x^*, 0)$. An approximation for the observation model can be written as

$$Y_{k+1} \approx G^r_{k+1}(x^*) + \partial G^r_{k+1}(X_{k+1} - x^*) + \nu^r_{k+1} + V_{k+1},$$

where ∂G_k^r is the Jacobian matrix of G_k^r evaluated at x^*.

Since smallest linearization error is achieved near the linearization point, the linearization point should be chosen such that it represents the best possible guess for the state based on the information available at current time. Hence, the linearization point for the evolution model is chosen to be $\widehat{X}_k^r$ and for the observation model it is chosen to be $\widetilde{X}_{k+1}^r$.

Assume that the initial state X_0 and the processes W_k and V_k in the accurate model (2.1) satisfy the same assumptions that are made in Section 3.2. A similar argument as in Section 3.1 results the following equations

$$\begin{aligned}
\widetilde{X}_{k+1}^r &= F_{k+1}^r(\widehat{X}_k^r, 0) + \mathbb{E}^{d_k}\left[\epsilon_{k+1}^r\right], && (3.17)\\
\widetilde{\Gamma}_{k+1}^r &= \partial_x F_{k+1}^r \widehat{\Gamma}_k^r \partial_x F_{k+1}^{r\,\mathrm{T}} + \partial_w F_{k+1}^r \Sigma_{k+1}^{w,r} \partial_w F_{k+1}^{r\,\mathrm{T}} + \mathrm{cov}^{d_k}(\epsilon_{k+1}^r), && (3.18)\\
K_{k+1}^r &= \widetilde{\Gamma}_{k+1}^r \partial G_{k+1}^{r\,\mathrm{T}} (\partial G_{k+1}^r \widetilde{\Gamma}_{k+1}^r \partial G_{k+1}^{r\,\mathrm{T}} + \mathrm{cov}^{d_k}(\nu_{k+1}^r) + \Sigma_{k+1}^v)^{-1}, && (3.19)\\
\widehat{X}_{k+1}^r &= \widetilde{X}_{k+1}^r + K_{k+1}^r (y_{k+1} - G_{k+1}^r(\widetilde{X}_{k+1}^r) - \mathbb{E}^{d_k}\left[\nu_{k+1}^r\right]), && (3.20)\\
\widehat{\Gamma}_{k+1}^r &= (I - K_{k+1}^r \partial G_{k+1}^r) \widetilde{\Gamma}_{k+1}^r. && (3.21)
\end{aligned}$$

For details, see Publication III. These equations can be used as an estimator for the reduced state X_k^r. It is to be noted that, if we neglect the terms in which ϵ_k^r and ν_k^r appear in equations (3.17)–(3.21), the equations correspond to the extended Kalman filter (cf. [2, Page 195]).

In the linear case, Equations (3.12)–(3.16) contained cross-covariance terms related to ϵ_k^r and ν_k^r. Similar terms also appear in the derivation of Equations (3.17)–(3.21) (see Publication III). However, in the nonlinear case the predictor and filter covariances given by Equations (3.18) and (3.21) may not be positive semidefinite matrices (i.e., proper covariance matrices) and the estimator may become unstable. Therefore the conditional cross-covariances are approximated with zero matrices in the derivation of Equations (3.17)–(3.21). This issue with further details is discussed in Section 3.4.

Temporal discretization

In Section 2.3 we discussed about the use of small time stepping in temporal discretization and constructed the evolution model (2.12) which corresponds to measurement times. To use the nonlinear recursive estimator presented in this section, we need to calculate the Jacobian matrices associated to this evolution model. These Jacobian matrices can be calculated as follows.

Assume that $\bar{F}_j$ are differentiable for all $j = 1, \ldots, \bar{N}$. Consequently, F_k are differentiable for all $k = 1, \ldots, N$. Denote the Jacobian matrices of F_k with respect to x and w by $\partial_x F_k$ and $\partial_w F_k$, respectively, and the Jacobian matrices of $\bar{F}_{kN_d+j}$ with respect to x and w by $\partial_x \bar{F}_j^k$ and $\partial_w \bar{F}_j^k$, respectively. Furthermore, denote $A_0^k = I$ and

$$A_j^k := \underbrace{\partial_x \bar{F}_{N_d}^k(x_{N_d-1}, w_{N_d}) \cdots \partial_x \bar{F}_{N_d-j+1}^k(x_{N_d-j}, w_{N_d-j+1})}_{j \text{ terms}}, \quad j = 1, \ldots, N_d.$$

Then the Jacobian matrices of F_{k+1} are given by the equations

$$\begin{aligned}
&\partial_x F_{k+1}(x, w) = A_{N_d}^k,\\
&\partial_{w_i} F_{k+1}(x, w) = A_{N_d-i}^k \partial_w \bar{F}_i^k(x_0, w_i), \quad i = 1 \ldots, N_d,\\
&\partial_w F_{k+1}(x, w) = [\partial_{w_1} F_{k+1}(x, w) \ \cdots \ \partial_{w_{N_d}} F_{k+1}(x, w)].
\end{aligned}$$

For details, see Publications III.

3.4 Computation of the statistics of ϵ_k^r and ν_k^r

In this section we will describe how the statistics for the approximation error terms are computed. More precisely, we determine the (approximative) conditional expectations, covariances and cross-covariances of ϵ_{k+1}^r and ν_{k+1}^r given $\mathrm{D}_k = d_k$. We consider the linear case first.

Linear model

We need to compute the conditional expectations and covariances of ϵ_k^r and ν_k^r and the conditional cross-covariances $\mathrm{cov}^{d_k}(\epsilon_{k+1}^r, X_k^r)$, $\mathrm{cov}^{d_k}(\epsilon_{k+1}^r, U_{k+1})$, $\mathrm{cov}^{d_k}(\nu_{k+1}^r, X_{k+1}^r)$ and $\mathrm{cov}^{d_k}(\nu_{k+1}^r, \widetilde{U}_{k+1})$. In the linear case the approximation error terms are images of the accurate state given by linear operations. Since the expectation (as an integral operator) commutes with other linear operators, it is straightforward to derive the exact equations for these quantities.

From the definition of ϵ_k^r,

$$\begin{aligned}
\mathbb{E}^{d_k}[\epsilon_{k+1}^r] &= (P_r A_{k+1} - A_{k+1}^r P_r)\mathbb{E}^{d_k}[X_k] + (P_r B_{k+1} - B_{k+1}^r)\Sigma_{k+1}^u, \\
\mathrm{cov}^{d_k}(\epsilon_k^r) &= (P_r A_{k+1} - A_{k+1}^r P_r)\mathrm{cov}^{d_k}(X_k)(P_r A_{k+1} - A_{k+1}^r P_r)^{\mathrm{T}} \\
&\quad + (P_r B_{k+1} - B_{k+1}^r)\Sigma_{k+1}^u (P_r B_{k+1} - B_{k+1}^r)^{\mathrm{T}}, \\
\mathrm{cov}^{d_k}(\epsilon_k^r, X_k^r) &= (P_r A_{k+1} - A_{k+1}^r P_r)\mathrm{cov}^{d_k}(X_k) P_r^{\mathrm{T}}, \\
\mathrm{cov}^{d_k}(\epsilon_k^r, U_{k+1}) &= (P_r B_{k+1} - B_{k+1}^r)\Sigma_{k+1}^u,
\end{aligned}$$

since U_{k+1} is independent of X_k and D_k. Similarly for ν_k^r we have

$$\begin{aligned}
\mathbb{E}^{d_k}[\nu_{k+1}^r] &= (C_{k+1} - C_{k+1}^r P_r)\mathbb{E}^{d_k}[X_{k+1}] + (D_{k+1} - D_{k+1}^r)\eta_{k+1}^{\widetilde{u}}, \\
\mathrm{cov}^{d_k}(\nu_{k+1}^r) &= (C_{k+1} - C_{k+1}^r P_r)\mathrm{cov}^{d_k}(X_{k+1})(C_{k+1} - C_{k+1}^r P_r)^{\mathrm{T}} \\
&\quad + (D_{k+1} - D_{k+1}^r)\Sigma_{k+1}^{\widetilde{u}} (D_{k+1} - D_{k+1}^r)^{\mathrm{T}}, \\
\mathrm{cov}^{d_k}(\nu_{k+1}^r, X_{k+1}^r) &= (C_{k+1} - C_{k+1}^r P_r)\mathrm{cov}^{d_k}(X_{k+1}) P_r^{\mathrm{T}}, \\
\mathrm{cov}^{d_k}(\nu_{k+1}^r, \widetilde{U}_{k+1}) &= (D_{k+1} - D_{k+1}^r)\Sigma_{k+1}^{\widetilde{u}}.
\end{aligned}$$

In principle, the conditional expectations $\mathbb{E}^{d_k}[X_k]$ and $\mathbb{E}^{d_k}[X_{k+1}]$ can be computed by using the accurate model (2.8). However, these terms depend on the measurements d_k and cannot be computed prior to any measurements. Furthermore, these terms are actually the filter estimates $\widehat{X}_k$ and $\widetilde{X}_{k+1}$ for the filtering problem related to the accurate model (2.1), see Section 3.1. Thus, if these terms are computed, it is meaningless to use the reduced model at all. For practical purposes, we have to approximate these conditional expectations with the conventional expectations, i.e., we choose $\mathbb{E}^{d_k}[X_{k+1}] \approx \mathbb{E}[X_k]$ and $\mathbb{E}^{d_k}[X_{k+1}] \approx \mathbb{E}[X_{k+1}]$.

We can also approximate the covariances $\mathrm{cov}^{d_k}(X_k)$ and $\mathrm{cov}^{d_k}(X_{k+1})$ with the respective conventional covariances. This is a safe choice in a way that the conditional variances are smaller than the conventional variances and therefore the uncertainty of the random variables is at least not underestimated. This approximation is not, however, imperative, since these conditional covariances do not depend on measurements (see Equations (3.4), (3.8) and (3.9)) and these terms can be computed prior any measurements are taken. On the other hand, if we approximate the conditional covariances with the conventional covariances, there is a risk that the filter covariance and the predictor covariances given by Equations (3.13) and (3.15) are not positive semidefinite. In spite

of all, based on the simulations in Publications I and II, the approximation of the conditional covariances with the conditional covariances seems to be viable. Actually, in the case of the simulation in Publication I (where these both approaches could be used), the difference in the results between these approaches was insignificant.

The conditional expectations and covariances of the state X_k can be computed recursively using the accurate evolution model (2.8):

$$\begin{aligned} \mathbb{E}[X_{k+1}] &= A_{k+1}\mathbb{E}[X_{k+1}] + B_{k+1}\mathbb{E}[U_{k+1}], \\ \mathrm{cov}(X_{k+1}) &= A_{k+1}\mathrm{cov}(X_k)A_{k+1}^{\mathrm{T}} + B_{k+1}\Sigma_{k+1}^u B_{k+1}^{\mathrm{T}} + \Sigma_{k+1}^w \end{aligned}$$

for all $k = 0, \ldots, N-1$ where Σ_{k+1}^w is the covariance of W_{k+1}.

Nonlinear model

In nonlinear case there are no similar explicit equations for the expectations, covariances and cross-covariances related to ϵ_k^r and ν_k^r as in the linear case. Instead, the approximative statistics for the error terms can be computed by using an ensemble of samples of these approximation errors.

At first, the conditional expectations and covariances of ϵ_{k+1}^r and ν_{k+1}^r are approximated with the conventional covariances, i.e., we choose $\mathbb{E}^{d_k}[\epsilon_{k+1}^r] \approx \mathbb{E}[\epsilon_{k+1}^r]$, $\mathrm{cov}^{d_k}(\epsilon_{k+1}^r) \approx \mathrm{cov}(\epsilon_{k+1}^r)$, $\mathbb{E}^{d_k}[\nu_{k+1}^r] \approx \mathbb{E}[\nu_{k+1}^r]$ and $\mathrm{cov}^{d_k}(\nu_{k+1}^r) \approx \mathrm{cov}(\nu_{k+1}^r)$. This corresponds to the approximation made in the linear case in which the conditional expectations and covariances of X_k and X_{k+1} are approximated with the conventional expectations and covariances. To avoid the filter and predictor covariances become improper covariance matrices, in the nonlinear case the conditional cross-covariances related to the approximation error terms are approximated with zero matrices (as already mentioned in Section 3.2). It is to be noted that, although it was not necessary to neglect these conditional cross-covariance in the linear case, that seems to be imperative in the nonlinear case. The main reason for this issue seems to be the linearizations made in the derivation of the filter recursion. Namely, if in the nonlinear case the cross-covariance matrices are not neglected, the covariance matrices can become indefinite even during the first recursion step when the approximations related to the conditional expectations and covariances of ϵ_k^r and ν_k^r are not effective (note that $\mathrm{cov}^{d_0}(\cdot)$ was the notation for the conventional covariance).

We generate an ensemble of samples from the family of random variables $\{X_0^r, X_k^r, W_k^r, \epsilon_k^r, \nu_k^r,\ k = 1, \ldots, N\}$ as follows. Let M be the number of samples. We draw a sample X_0^j $(j = 1, \ldots, M)$ from the distribution of the initial state X_0 and put $X_0^{r,j} = P_r X_0^j$. Then for each $k = 1, \ldots, N$ we carry out the following steps:

1. draw W_k^j from the distribution of W_k and put $W_k^{r,j} = P_{\mathrm{w}} W_k^j$;
2. compute $X_k^j = F_k(X_{k-1}^j, W_k^j)$ and put $X_k^{r,j} = P_r X_k$;
3. compute $\epsilon_k^{r,j} = X_k^{r,j} - F_k^r(X_{k-1}^{r,j}, W_k^{r,j})$ and $\nu_k^{r,j} = G_k(X_k^j) - G_k^r(X_k^{r,j})$.

There are cases in which we can treat the evolution model conditioned on the initial state as a deterministic model and simplify the procedure by neglecting the state noise (i.e., by choosing $W_k^j = 0$). This can be done if we can assume that the evolution model of the accurate state is a correct model for the problem so that the effects of the state noise are negligible.

The approximate expectations and covariances are computed as the respective sample means and covariances by using the equations

$$\mathbb{E}[\epsilon_k^r] \approx \mu_M^\epsilon := \frac{1}{M}\sum_{j=1}^{M}\epsilon_k^{r,j}, \qquad \mathrm{cov}(\epsilon_k^r) \approx \frac{1}{M-1}\sum_{j=1}^{M}(\epsilon_k^{r,j}-\mu_M^\epsilon)(\epsilon_k^{r,j}-\mu_M^\epsilon)^{\mathrm{T}},$$

$$\mathbb{E}[\nu_k^r] \approx \mu_M^\nu := \frac{1}{M}\sum_{j=1}^{M}\nu_k^{r,j}, \qquad \mathrm{cov}(\nu_k^r) \approx \frac{1}{M-1}\sum_{j=1}^{M}(\nu_k^{r,j}-\mu_M^\nu)(\nu_k^{r,j}-\mu_M^\nu)^{\mathrm{T}}$$

for every $k = 1, \ldots, N$. The approximative covariance matrices may be rank-deficient, but this is not a problem due to the fact that the covariance of the measurement noise Σ_k^v is usually positive definite and therefore the matrix which has to be inverted for the Kalman gain is non-singular.

Finally, we note that the number of samples M may not have to be high compared to the dimension of the state vector or the number of samples. It has turned out that in practice the suitable accuracy for the statistics of the approximation errors can be achieved using relative small number of measurement [35, 45]. This property, however, is not studied in this thesis. Instead, M is chosen to be relatively high such that the increment of M does not essentially change the estimates.

3.5 Hybrid filter

As already mentioned in Section 3.1, the information filter form of the KF recursion is not computationally efficient if the dimension of measurement vector is large compared to the dimension of the state vector. The same applies to the methods presented in Sections 3.2 and 3.3. In this section we present a modification of the methods for the case in which the dimension of the measurement vector is high. The modification is a hybrid form of the innovation and information filter forms.

The main motivation for the extension is related to the problem described in Publications IV–V. In this problem the measurements are magnetic resonance thermal images [33] that are usually of the size of 128x128 or higher. Hence, when this problem is treated as a nonstationary parameter estimation problem as in Publication V, the measurement noise covariance Σ_{k+1}^v (among others) contains 128^4 elements and the computation of the Kalman gain matrix K_{k+1}^r is prohibitively complex.

Since the resulting state space model in Publication V is nonlinear, we consider only the nonlinear case. The information filter described in Section 3.1 was expressed in terms of the inverse of the matrix A_k. However, in the nonlinear case there is no term which corresponds to A_k^{-1} and thus similar equations as in the information filter cannot be found. Instead, we confine ourself by modifying the observation update equations (3.14)–(3.16) using the Sherman-Morrison Woodbury formula.

The basic idea of the modification is to write the covariance $\mathrm{cov}(\nu_{k+1}^r)$ in the form $\mathrm{cov}(\nu_{k+1}^r) = \Xi_{k+1}\Xi_{k+1}^{\mathrm{T}}$. This is due to the fact that the covariance estimate can be written as an outer product in the first place, that is, $\mathrm{cov}(\nu_k^r) = M^{-1}AA^{\mathrm{T}}$ where A is a matrix whose jth column is $\nu_k^j - \bar{\nu}_k$. Thus Ξ can be chosen to be $\Xi = M^{-1/2}A$. It is to be noted that the dimension of the matrix Ξ_{k+1} is typically significantly smaller than the covariance $\mathrm{cov}(\nu_k^r)$.

An application of the SMW formula to Equation (3.19) gives the following equation for the Kalman gain

$$K_{k+1}^r = \Psi_{k+1}\partial G_{k+1}^{r\,\mathrm{T}}{\Sigma_{k+1}^v}^{-1} - \Psi_{k+1}\Phi_{k+1}^{\mathrm{T}}\Lambda_{k+1}\Xi_{k+1}^{\mathrm{T}}{\Sigma_{k+1}^v}^{-1} \tag{3.22}$$

where the matrices Λ_{k+1}, Φ_{k+1} and Ψ_{k+1} are given by

$$\begin{aligned}
\Lambda_{k+1} &= (\Xi_{k+1}^{\mathrm{T}} {\Sigma_{k+1}^{v}}^{-1} \Xi_{k+1} + I)^{-1}, \\
\Phi_{k+1} &= \Xi_{k+1}^{\mathrm{T}} {\Sigma_{k+1}^{v}}^{-1} \partial G_{k+1}^{r}, \\
\Psi_{k+1} &= [{\widetilde{\Gamma}_{k+1}^{r}}^{-1} + \partial G_{k+1}^{r\,\mathrm{T}} {\Sigma_{k+1}^{v}}^{-1} \partial G_{k+1}^{r} - \Phi_{k+1}^{\mathrm{T}} \Lambda_{k+1} \Phi_{k+1}]^{-1}.
\end{aligned}$$

The equation (3.22) can be used with Equations (3.20)–(3.21) to compute the filter estimates. The covariance of the measurement noise is often a diagonal matrix and thus can be inverted easily. Hence, the largest full matrix which has to be inverted is of the size $n \times n$ or $M \times M$, not of the size $m \times m$. The computationally most demanding tasks are the computation of the inverse of $\widetilde{\Gamma}_{k+1}^{r}$ and the matrix Ψ_{k+1}. For details, see Publication V.

Finally, we consider a special case in which the mapping G_{k+1}^{r} is linear. This kind of a situation occurs in the simulation presented in Publication V, in which G_{k+1}^{r} is an interpolation matrix from the computational mesh to the measurement grid. Substitution of (3.22) to the observation update equations (3.20)–(3.21) gives

$$\begin{aligned}
\widehat{X}_{k+1}^{r} &= \widetilde{X}_{k+1}^{r} + \Psi_{k+1} G_{k+1}^{r\,\mathrm{T}} {\Sigma_{k+1}^{v}}^{-1} z_k - \Psi_{k+1} G_{k+1}^{r\,\mathrm{T}} {\Sigma_{k+1}^{v}}^{-1} G_{k+1}^{r} \widetilde{X}_{k+1}^{r} \\
&\quad - \Psi_{k+1} \Phi_{k+1}^{\mathrm{T}} \Lambda_{k+1} \Xi_{k+1}^{\mathrm{T}} {\Sigma_{k+1}^{v}}^{-1} z_k + \Psi_{k+1} \Phi_{k+1}^{\mathrm{T}} \Lambda_{k+1} \Phi_{k+1} \widetilde{X}_{k+1}^{r}, \\
\widehat{\Gamma}_{k+1}^{r} &= \widetilde{\Gamma}_{k+1}^{r} - \Psi_{k+1} G_{k+1}^{r\,\mathrm{T}} {\Sigma_{k+1}^{v}}^{-1} G_{k+1}^{r} \widetilde{\Gamma}_{k+1}^{r} + \Psi_{k+1} \Phi_{k+1}^{\mathrm{T}} \Lambda_{k+1} \Phi_{k+1} \widetilde{\Gamma}_{k+1}^{r},
\end{aligned}$$

where $z_k = y_{k+1} - \mathbb{E}^{d_k}[\nu_{k+1}^{r}]$. This form is computationally more efficient compared to Equations (3.22), (3.20) and (3.21). However, the multiplication order should be chosen carefully.

3.6 Synopsis

We have derived an estimation scheme for nonstationary problems taking into account approximation errors in state-space models. In simplicity, the procedure to build up the estimation system is as follows.

1. At first, we need to find the mappings F_k, G_k, F_k^r and G_k^r associated the state space models. In PDE induced problems, these mapping are usually constructed by using some numerical scheme such as the finite difference or the finite element method (FEM). The sufficiently accurate model can be achieved by using fine spatial and temporal discretization and for the reduced model spatial and temporal discretization can be relatively sparse. The mapping P_r can be chosen to be the interpolation mapping between the computational meshes.
2. The expectation and the covariance of the initial state have to be specified. As usually, these can be determined based on prior information available for the initial state. Furthermore, the covariances of measurement noise and the state noise have to be specified. The measurement noise covariance is typically obtained by carefully analyzing the measurement system. The state noise covariance is often chosen to be a scaled identity matrix $\sigma_W^2 I$ where a constant σ_W is chosen empirically. The state noise covariance can also be estimated by using simulations, see for example [62].
3. The statistics of the approximation error terms has to be computed. This can be done as described in Section 3.4.

4. Finally, the estimates for the reduced state X_k^r can be computed recursively by using Equations (3.12)–(3.16) (linear case) or (3.17)–(3.21) (nonlinear case). If the number of measurements is high when compared to the dimension of the state vector, the hybrid filter form described in Section 3.5 can be used.

This method is computationally more demanding compared to the use of the reduced model (2.2) with conventional Kalman filtering techniques. However, the additional task relates to the computation of the statistics of the approximation error terms and that task can be carried out when the measurement system is set up before any measurements. During the run time the proposed method is not essentially more demanding than to the KF recursion with the reduced model.

Chapter IV

Review on the results

In this chapter we give a brief review of the simulations carried out in Publications I–V and summarize the results given by these simulations. In Section 4.1 we present a linear state space estimation problem described in Publication I, in which a temperature distribution in a one–dimensional (1D) rod is determined based on temperature measurements. In Section 4.2 we consider a process tomography problem presented in Publication II in which a concentration distribution of flow in a pipe is monitored. In this problem we use an approach in which the state space of the accurate model is infinite–dimensional.

The simulation in Publication III is reviewed in Section 4.3. In this simulation the coefficients of the 1D thermal equation are estimated as distributed parameters based on temperature measurements. In Section 4.4 we consider the estimation of heterogeneous thermal properties in tissue using ultrasound induced heating and MR temperature measurements. The measurement procedure has been introduced in Publication IV while the state space approach has been applied to the problem in Publication V.

4.1 Temperature prediction with the 1D thermal equation (I)

We consider the following temperature prediction problem. We can control the temperature of one end of a 1D rod while the other end is insulated. The rod is modelled as the unit interval $\Omega = [0, 1]$ in which the temperature distribution u satisfies the 1D heat equation

$$\frac{\partial u}{\partial t} = \frac{\partial}{\partial x}\left(a\frac{\partial u}{\partial x}\right) \qquad \text{in } (0, t_{\mathrm{F}}) \times (0, 1)$$

with the initial condition $u(0, \cdot) = 0$ and the boundary conditions $\frac{\partial u}{\partial x}(t, 0) = 0$ and $u(t, 1) = c\sin(\omega t)$ for $t \in [0, t_{\mathrm{F}}]$. The coefficients a, c and ω are assumed to be known positive constants. The problem is to determine the temperature distribution u based on direct temperature measurements taken at given points.

It is to be noted that, since the coefficients in the model are known, we would not need any measurements to know the temperature evolution. However, in this case we use the proposed state estimation approach to assess how well this approach allows us to reduce state and increase time stepping in temporal integration.

A state space model for the problem is constructed by using the finite element method

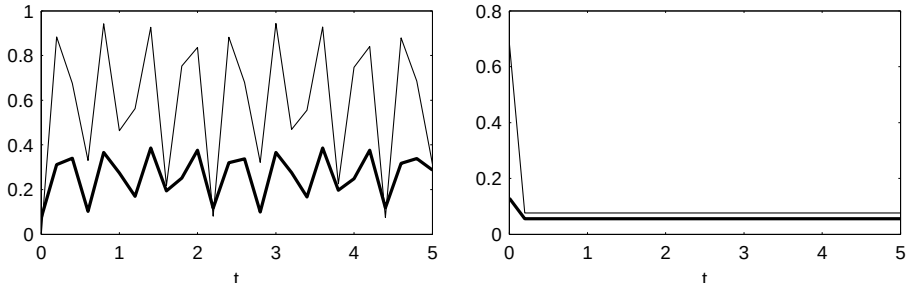

Figure 4.1: Left: The norm of the expectation of ϵ_k^r (bold line) and ν_k^r (thin line). Right: The square-root of the trace of the covariances of ϵ_k^r (bold line) and ν_k^r (thin line).

(FEM) with the linear basis functions while the temporal integration is carried out by the implicit Euler method. The accurate and reduced models are constructed by using different finite element (FE) meshes in spatial discretization and different time steps in temporal integration. The fine mesh of the accurate model includes the nodes of the sparse mesh used for the reduced model. Hence, the mapping P_r can be chosen to be a binary matrix so that P_r^{T} maps the nodes of the sparse mesh to the fine mesh. The simulated data is computed from the analytic solution of u by adding Gaussian noise. The construction of the models and the computation of estimates and the simulated data are described in detail in Publication I.

Results

The norms of the expectations and the square-root of the trace of the covariances of the approximation error terms ϵ_k^r and ν_k^r are shown in Figure 4.1. The time average of $\|\mathbb{E}[\epsilon_k^r]\|^2 + \operatorname{Tr}\operatorname{cov}(\epsilon_k^r) = 8.2 \cdot 10^{-2}$ which represents the energy of the errors due to discretization. When compared to $\operatorname{Tr}\Sigma_k^{w,r} = 3.2 \cdot 10^{-7}$, we may see that the approximation errors dominates over other errors in the evolution model. Hence, if the effects of the approximation errors in the evolution model were neglected, the predictor covariance could be too small, i.e., the accuracy of the predictor estimate would be exaggerated. This would lead to underestimation of the accuracy of the measurements and therefore to loss of information. Furthermore, as can be seen from Figure 4.2, the energy of the approximation errors is also highly unevenly distributed.

In the case of the observation model the time average of $\|\mathbb{E}[\nu_k^r]\|^2 + \operatorname{Tr}\operatorname{cov}(\nu_k^r) = 0.46$ which should be compared to $\operatorname{Tr}\Sigma_k^v = 0.40$. In this case the level of the energy of the approximation errors are of the same order of magnitude as the energy of measurement errors. However, also in this case the energy of the approximation errors are unevenly distributed and near the boundary, where the temperature changes are greatest, the energy is significantly higher than the standard deviation of the energy of measurement errors.

Three estimates are computed: one using the enhanced error model (2.11), one using the reduced model without approximation errors taken into account (i.e., by using the stochastic version of the reduced model (2.9) with the KF recursion) and the last is an estimate for the accurate state X_k using the accurate model (2.8) with the KF recursion.

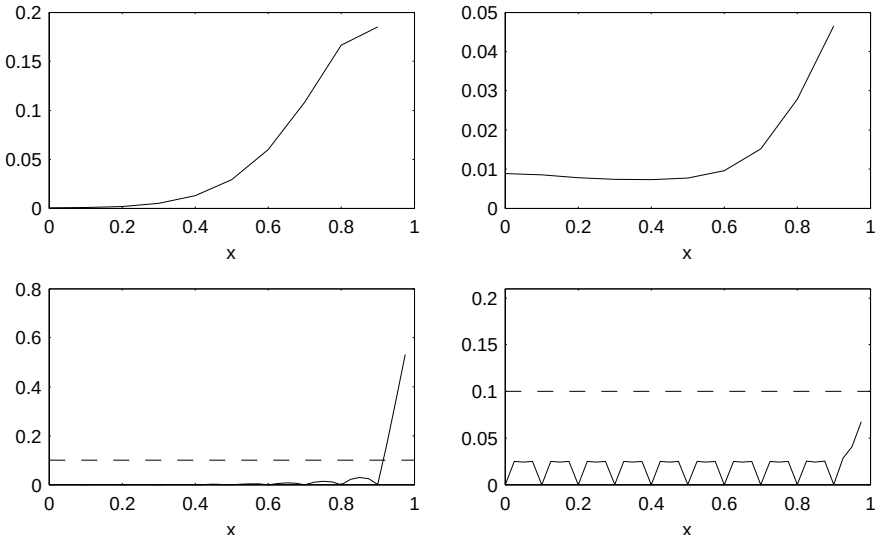

Figure 4.2: The distribution of the approximation errors: the square-root of the time average of $\mathbb{E}[\epsilon_k^r]^2$ (top-left) and $\mathbb{E}[\nu_k^r]^2$ (bottom-left) and the square-root of the time average of the diagonal elements of $\mathrm{cov}(\epsilon_k^r)$ (top-right) and $\mathrm{cov}(\nu_k^r)$ (bottom-right). The dashed line on the figures below corresponds to the standard deviation of measurement error.

The computed estimates for the final state $t = 5$ are shown in Figure 4.3. The results show that the estimates computed using the enhanced error model are significantly more accurate compared to the estimates computed using the reduced model. The results for the proposed method are essentially as good as with the accurate model.

One of the major benefits of the statistical framework for inverse problems in general is that reliable estimates for the errors can be computed. The computed confidence intervals for the estimates are also shown in Figure 4.3. As confidence intervals we use the square-roots of the diagonal elements of the filter covariance which correspond to the standard deviation of the estimation error. It can be seen that the error estimates computed using the reduced model correspond poorly to the true error. Instead, the error estimates computed using the enhanced error model conform well to the actual estimation errors. It is to be noted that the use of reduced models with conventional error models typically provides over-optimistic estimates for the accuracy [35].

4.2 Concentration distribution monitoring in process tomography (II)

We consider the monitoring of the concentration distribution of a given substance in fluid moving in a pipe based on indirect observations. We model the flow with the stochastic 1D convection-diffusion equation which is suitable for rotationally symmetrical concentration distributions.

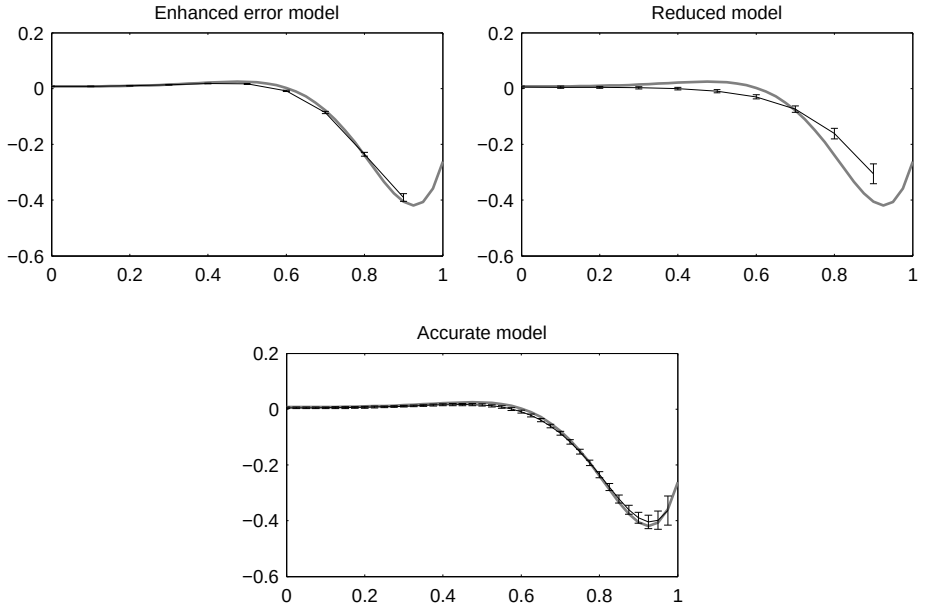

Figure 4.3: The computed estimates for the final state $t = 5$ with computed confidence intervals. The gray lines correspond to the analytic solution.

Denote by $L^2(\mathbb{R})$ and $H^2(\mathbb{R})$ the Lebesgue space and the Sobolev space on $\mathbb{R}$ and denote by $(\cdot,\cdot)$ the inner product in $L^2(\mathbb{R})$. Let X be an $L^2(\mathbb{R})$-valued stochastic process representing concentration distribution in the pipe. We model the evolution of the concentration distribution by the stochastic initial value problem

$$\begin{cases} dX(t) = AX(t)\mathrm{d}t + \mathrm{d}W(t), & 0 < t \leq t_{\mathrm{F}}, \\ X(0) = X_0 \end{cases} \tag{4.1}$$

where X_0 is an $L^2(\mathbb{R})$-valued Gaussian random variable, W is an $L^2(\mathbb{R})$-valued Wiener process and $A : H^2(\mathbb{R}) \to L^2(\mathbb{R})$ is the convection–diffusion operator given by

$$(Af)(x) = \frac{\mathrm{d}}{\mathrm{d}x}\left(\kappa(x)\frac{\mathrm{d}}{\mathrm{d}x}f(x)\right) - v(x)\frac{\mathrm{d}}{\mathrm{d}x}f(x), \quad x \in \mathbb{R}, \tag{4.2}$$

where κ is the diffusion coefficient and v is the velocity of the flow. The term Wiener process refers here to a generalization of the Brownian motion to a Hilbert space ($L^2(\mathbb{R})$ in this case) which covariance is a positive self-adjoint trace class operator. The term $\mathrm{d}W(t)$ in (4.1) represents uncertainties in the model. For a general reference to infinite–dimensional stochastic processes and stochastic differential equations, see [58].

For simplicity, the diffusion and the velocity are assumed to be known constants such that $\kappa > 0$. The choice of the covariance of the Wiener process W and the distribution of the initial state X_0 is described in [56] and Publication II.

The measurements are given by the equation

$$Y_k = CX(t_k) + V_k, \quad k = 1, \ldots, N,$$

where t_k are measurement times, V_k is measurement noise and the operator $C : L^2(\mathbb{R}) \to \mathbb{R}^m$ is given by

$$(Cf)_p = (f, \varphi_p) \quad \text{with} \quad \varphi_p(x) = \frac{1}{2w} \exp\left(-\frac{|x - x_p|}{w}\right)$$

for all $p = 1, \ldots, m$, where $x_1, \ldots, x_m$ are measurement points and $0 < w < 1$.

We use semigroups to construct the accurate state space. For the semigroup theory, see for example [52, 22, 28]. The convection–diffusion operator A generates an analytic semigroup $\{S(t)\}_{t \geq 0}$. The accurate state space model is given by this semigroup by

$$\begin{cases} X_{k+1} = S(\Delta_{k+1})X_k + W_{k+1}, & k = 0, \ldots, N-1, \\ Y_k = CX_k + V_k, & k = 1, \ldots, N, \end{cases} \tag{4.3}$$

where $X_k := X(t_k)$, $\Delta_{k+1} := t_{k+1} - t_k$ and the state noise W_{k+1} is given by

$$W_{k+1} = \int_{t_k}^{t_{k+1}} S(t_{k+1} - s)\mathrm{d}W(s)$$

for all $k = 0, \ldots, N-1$. The explicit form of the semigroup can be found by solving the convection diffusion equation (4.1) without the stochastic term $\mathrm{d}W(t)$, which is a deterministic initial value problem. The deterministic problem can be solved, for example, using Itô diffusions and the Feynman-Kac formula [50]. For the explicit form of the semigroup and other details, see [56] and Publication II.

It is to be noted that the realizations of the accurate state X_k are in $L^2(\mathbb{R})$ which is infinite–dimensional. To use model (4.3) in numerical calculations, the model has to be approximated in a finite–dimensional subspace.

Let $m \in \mathbb{N}$ and put $r = 2m^2$. For $j = 1, \ldots, r$, define functions ψ_j^m by

$$\psi_j^m(t) = \begin{cases} \sqrt{m}, & \text{if } \frac{j-1}{m} - m \leq t \leq \frac{j}{m} - m, \\ 0, & \text{otherwise.} \end{cases}$$

Then $\mathcal{V}_m := \operatorname{span}\{\psi_j^m,\ j = 1, \ldots, r\}$ is a finite–dimensional subspace of $L^2(\mathbb{R})$ and $\{\psi_j^m\}_{j=1}^r$ is its orthonormal basis. We identify the subspace $\mathcal{V}_m$ with $\mathbb{R}^r$ by using the coordinates in this basis and treat the orthogonal projection of X_k to $\mathcal{V}_m$ as the discretized version of X_k. More precisely, the reduced state is an $\mathbb{R}^r$-valued random variable $X_k^r := P_r X_k$ where the mapping P_r is

$$P_r : L^2(\mathbb{R}) \mapsto \mathbb{R}^r, \quad f \mapsto ((f, \psi_1^m), \ldots, (f, \psi_r^m))^{\mathrm{T}}.$$

The elements of the matrices A_k^r and C_k^r in the reduced model are

$$(A_k^r)_{ij} := (S(\Delta_k)\psi_j^m, \psi_i^m) \quad \text{and} \qquad (C_k^r)_{pj} := \left(\psi_j^m, \varphi_p\right).$$

for all $k = 1, \ldots, N$, $i, j = 1, \ldots, r$ and $p = 1, \ldots, m$.

The simulated data is generated by drawing a sample from the joint distribution of $X_0^r, \ldots, X_N^r$ and $Y_1 \ldots, Y_N$. This distribution is Gaussian and its mean and covariance can be calculated. For details, see Publication II.

Results

In this case the time average of $\|\mathbb{E}[\epsilon_k^r]\|^2 + \operatorname{Tr}\operatorname{cov}(\epsilon_k^r) = 0.0310$ which is of an order of magnitude higher than $\operatorname{Tr}\Sigma_k^{w,r} = 0.0030$. Thus also in this simulation the effects of the discretization errors are more significant than of other errors in the evolution model. The time average of $\|\mathbb{E}[\nu_k^m]\|^2 + \operatorname{Tr}\operatorname{cov}(\nu_k^m) = 0.0011$ which is rather insignificant compared to $\operatorname{Tr}\Sigma_k^v = 0.1000$. Hence, in this simulation the reduced observation model is probably sufficiently accurate and the effects of the term ν_k^m may not be significant. However, it is to be noted that, if the measurements are very accurate, the approximation error in the observation model can also be significant.

Three estimates are computed: one using the enhanced error model, one using the reduced model without approximation error taken into account and one using the accurate model. However, although in Section 4.1 the estimate computed using the accurate model was the filtering solution for the accurate state X_k, in this case it is easier to compute an exact filtering solution (or the true conditional distribution) for the reduced state X_k^r due to the infinite–dimensionality of the accurate model. The mean and the covariance of this conditional distribution can be calculated analytically, for example, using [35, Theorem 3.5]. In this case it is feasible to compute the inverse of the covariance of the stacked measurement vector D_k in practice due to the small number of measurements. For details, see Publication II.

The computed estimates and the absolute errors (the absolute value of the difference between the estimate and the true solution) are shown in Figure 4.4 and the estimates with confidence intervals for the final state $t = 10$ are shown in Figure 4.5. The results show that, as in Section 4.1, the accuracy of the estimates computed using the enhanced error model is almost as good as the accuracy of the true conditional expectation. Furthermore, the error estimates provide a rather good assessment of the errors. On the contrary, the accuracy of the estimates computed using the reduced model is much worse and the confidence intervals correspond poorly to the actual error.

4.3 Parameter estimation in 1D thermal equation (III)

We consider a situation which is similar to the first simulation. The temperature in a 1D rod is modelled with a PDE

$$\frac{\partial u}{\partial t} = \frac{\partial}{\partial x}\left(a\frac{\partial u}{\partial x}\right) - bu \qquad \text{in } (0, t_{\mathrm{F}}) \times (0, 1) \tag{4.4}$$

with the initial condition $u(0, \cdot) = 0$ and the boundary conditions $\frac{\partial u}{\partial x}(t, 0) = 0$ and $u(t, 1) = c\sin(\omega t)$ for $t \in [0, t_{\mathrm{F}}]$. In some applications the second term on right represents thermal leakage or thermal dissipation. The coefficients c and ω are assumed to be known positive constants. In contrast with Section 4.1, the coefficients a and b are assumed to be unknown distributed parameters.

We have measurements from u given by the equation

$$(Y_k)_p = A_0 \exp\left(A_1 + \frac{A_2}{u_{k,p}} + \frac{A_3}{u_{k,p}^2} + \frac{A_4}{u_{k,p}^3}\right) + (V_k)_p \tag{4.5}$$

where $u_{k,p}$ is the temperature in Kelvin at a time instant t_k ($k = 1, \ldots, N$) in a measurement point x_p ($p = 1, \ldots, m$), V_k is measurement noise and A_0, A_1, A_2, A_3 and A_4 are known constants. This type of an equation is typical for NTC thermistors [8].

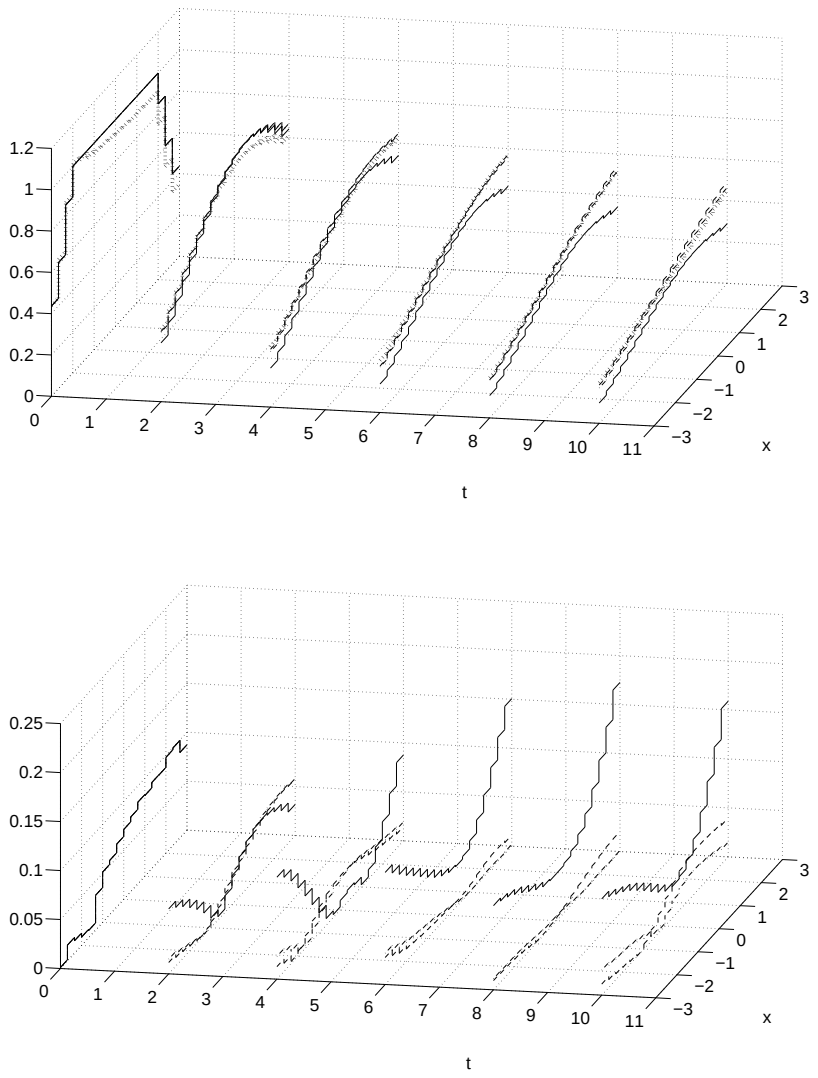

Figure 4.4: The computed estimates (top) and absolute errors (bottom): the estimate that is computed using the enhanced error model (−−), the estimate that is computed using the reduced model and the real conditional expectation (−·). The real solution is also shown on top (··).

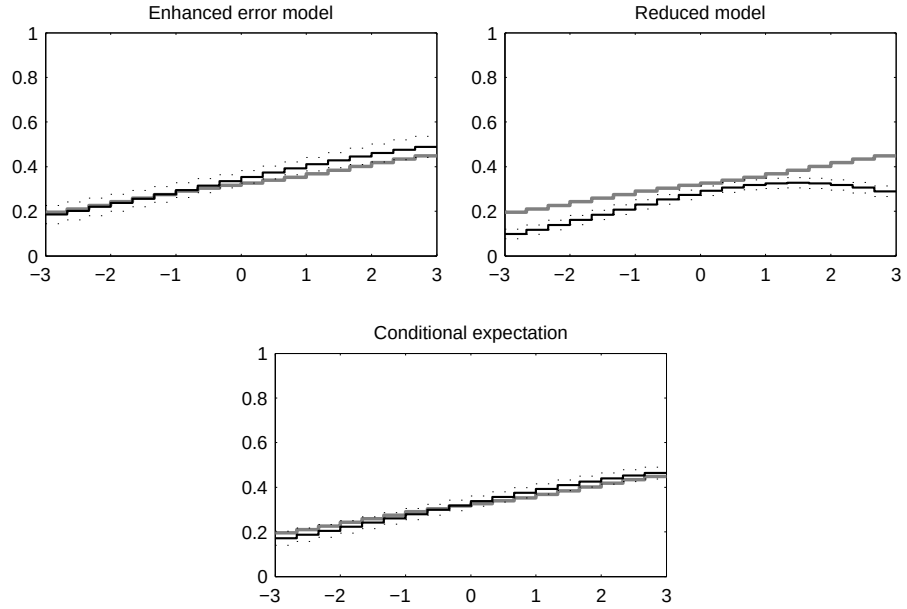

Figure 4.5: The computed estimates for the final state $t = 10$ (black lines) with the computed confidence intervals $(\cdot\cdot)$. The gray lines correspond to the exact solution.

The problem is to estimate the distributed coefficients a and b based on measurements $Y_1, \ldots, Y_N$. For the simulation, we choose the true coefficients a and b to be constants. In this case the simulated measurements can be computed from the analytic solution of the u.

Similarly as in Section 4.1, the state space models are constructed by using FEM and implicit Euler method with different finite element meshes and temporal discretization levels for the accurate and reduced models. The coefficients a and b are approximated in a piecewise constant basis. The coefficients are estimated by using the adaptive estimation approach described in Section 2.4. The augmented state vector is $X_k^{\mathrm{A}} = (X_k, a_k, b_k)$ where a vector X_k represents the temperature in the FE basis. The coefficients a and b are assumed to be temporally invariant so that the evolution models for these coefficients are chosen to be

$$a_{k+1} = a_k \quad \text{and} \quad b_{k+1} = b_k, \quad k = 0 \ldots, N-1.$$

Note that, since the evolution models for a and b do not contain state noises, the statistics of these processes is determined by their prior distributions.

In this case both the evolution model and the observation models are nonlinear. Hence the nonlinear extension represented in Section 3.3 is used. The computations are described in detail in Publication III.

Results

In this case the energy of errors is distributed similarly as in the previous simulation. The time average of $\|\mathbb{E}[\epsilon_k^r]\|^2 + \operatorname{Tr}\operatorname{cov}(\epsilon_k^r) = 0.419$ which is much higher than $\operatorname{Tr}\Sigma_k^w = 0.001$. The time average of $\|\mathbb{E}[\nu_k^r]\|^2 + \operatorname{Tr}\operatorname{cov}(\nu_k^r) = 0.051$ which, compared to $\operatorname{Tr}\Sigma_k^v = 3.61$, is not significant. Thus the effects of the approximation errors in the evolution model are significant but not very necessarily in the observation model.

Again, three estimates are computed: one using the enhanced error model, one using the reduced model and one for the accurate augmented state using the accurate state space model. The computed estimates and confidence intervals for the coefficients a and b are shown in Figure 4.6. These estimates are the components of the filter estimates for the augmented final state $X_N^{\mathrm{A},r}$ (or X_N^{A}) corresponding to a and b and the confidence limits are the square roots of the corresponding diagonal elements of the filter covariances.

The results are similar as in the previous simulations. The estimates computed using the enhanced error model are only slightly less accurate than the estimates computed using the accurate model. Furthermore, the confidence limits correspond well to the actual errors. On the contrary, the accuracy of the estimates computed using the reduced model is poorer and the confidence intervals are also highly over-optimistic. It is to be noted that the derivation of the EKF recursion contains linearizations and approximations which may cause that the confidence limits are over-optimistic and the actual errors are several times higher than the computed confidence limits. However, this seems not to be a major problem in this case when the enhanced error model is used.

4.4 Estimation of the thermal parameters of tissue (IV–V)

As the last application we consider the determination of the thermal conductivity and perfusion coefficient of tissue. In Publication IV we have described an approach to determine these coefficients by using ultrasound transducers and magnetic resonance (MR) scanner. Similar approaches to determine homogeneous thermal coefficients of tissue are described in [14, 67].

The motivation of the study in Publication IV is related to ultrasound surgery. In US surgery the aim is to destroy target tissue (a tumor) by using high intensity focused ultrasound [16]. This ability to destroy tissue is based on the ultrasound absorption which causes temperature elevation into tissue.

US surgery has been clinically proven to be a feasible treatment modality in a number of different situations [32, 68, 61, 66, 13]. US surgery treatment has been carried out by producing sharply focused temperature elevation into tissue. By moving this focal spot the whole target tissue is scanned. However, this method has also drawbacks. For example, the overall treatment time is often long since the focal spot is small and thus it takes a long time to scan the whole target volume.

Various other approaches for US surgery have been recently studied. For example, US surgery can be carried out by using a system of transducers called a *phased array*. The phased arrays allow us to increase the size of the focal spot and move the position of the each position electrically by changing the amplitudes and phases of individual transducers. The treatment planning for US surgery using phased arrays can be done with several techniques. For example, applications of model-based optimization methods have been studied in [48, 19, 67].

To implement a model based treatment planning system, the thermal and acoustic properties have to be known. Although the tissue properties have been widely studied and

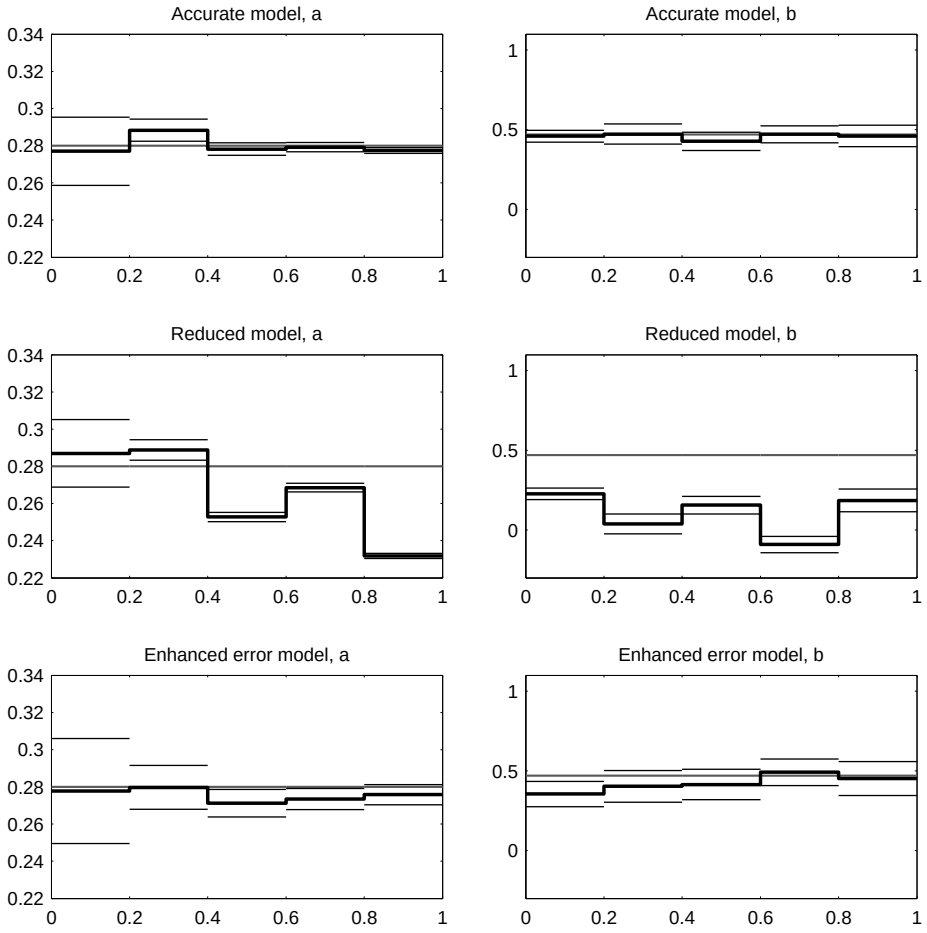

Figure 4.6: The computed estimates for the coefficients a and b at the final time $t = 5$ with computed confidence intervals. The gray lines correspond to the actual coefficients.

average values have been collected for several different tissues, some properties depend strongly on the physiological state of the tissue, especially on the water content. Thus, it is reasonable to determine the thermal and acoustic properties of tissue for each patient separately before the actual ultrasound treatment.

A magnetic resonance (MR) scanner can be used in several tasks during ultrasound treatment. For example, after the treatment, the MR images can be used to ensure that the whole target tissue is ablated [49, 70]. An MR scanner can also be used to measure the temperature distribution of tissue during the treatment [51]. This MR temperature imaging is based on measuring differences of factors which are temperature dependent. The most widely used factor is the proton resonance frequency shift which is related to chemical interactions of the hydrogen bonds [33]. In US surgery, the MR thermal imaging can be used to ensure the correct location of a focal spot [49]. Furthermore, MR temperature data can also be used as the system feedback for the model-based treatment planning, see for example [47].

The overview of the approach described in IV is as follows. The same ultrasound transducers, which are eventually to be used in the US surgery, are used to inflict small nondestructive temperature changes into tissue. This temperature evolution is monitored using the MR thermal imaging and the thermal properties are estimated from these temperature measurements using the maximum a posteriori estimation scheme. In Publication V this thermal property estimation problem is treated as a nonstationary parameter estimation problem (see Section 2.4) and the problem is solved using the state estimation technique presented in this thesis. In this section we only summarize the results given in Publication V.

Mathematical models

Let $\Omega \subset \mathbb{R}^{2,3}$ be a bounded domain corresponding to (a part of) the human body. Heat transfer in tissue is modelled using Pennes' bioheat equation [53]

$$\rho C_{\mathrm{T}} \frac{\partial T}{\partial t} = \nabla \cdot (\kappa \nabla T) - w_{\mathrm{B}} C_{\mathrm{B}} (T - T_{\mathrm{A}}) + Q \quad \text{in } (0, t_{\mathrm{F}}) \times \Omega, \tag{4.6}$$

where T is the temperature, T_{A} is the temperature of arterial blood, ρ is the density of the medium, κ is the thermal conductivity, C_{T} and C_{B} are the heat capacity of the tissue and blood, respectively, w_{B} is the blood flow rate and Q is the heat source. For ultrasound absorption, the heat source Q can be written as [16, 54]

$$Q = \frac{\alpha |P|^2}{\rho c}$$

where P is the ultrasound pressure field, α is the absorption coefficient and c is the speed of sound.

We endow the problem with the initial and boundary conditions

$$\begin{aligned} T(0, \cdot) &= T_{\mathrm{A}} \qquad \text{in } \Omega, \\ T(t, x) &= T_{\mathrm{A}} \qquad \text{if } x \in \partial\Omega,\ 0 \le t \le t_{\mathrm{F}}. \end{aligned}$$

These conditions involve an assumption that the temperature of the arterial blood is same as body temperature. Thus T_{A} can also be considered as ambient temperature.

We denote $\beta = w_{\mathrm{B}} C_{\mathrm{B}}$ and call β the perfusion coefficient. All coefficients in Eq. (4.6) are assumed to be distributed parameters. However, we divide the domain into smaller subdomains in which the coefficients are assumed to be constants. This segmentation

can be formed, for example, by using MRI images so that each type of tissue forms its own subdomain. Furthermore, the parameters are assumed to be constant with respect to temperature, which is warranted since only small temperature changes are inflicted [71, 3, 74]. The coefficients which are (partially) unknown and are being estimated in this simulation, are κ and β.

The ultrasound field P is assumed to time-harmonic so that it can be expressed as $P(t,x) = p(x)e^{\mathrm{i}2\pi ft}$ where f is the frequency of the wave field. This is warranted since the period of vibration is typically five orders of magnitude shorter than the time for observable temperature changes in tissue. The spatially dependent part p is modelled using the Helmholtz equation

$$\nabla \cdot \left(\frac{1}{\rho}\nabla p\right) + \frac{k^2}{\rho}p = 0, \tag{4.7}$$

where k is the wave number and ρ is the density of the medium. In an absorbing medium, the wave number is of the form $k = 2\pi f/c + \mathrm{i}\alpha$ [9]. The solution of the Helmholtz equation is computed using the ultraweak variational formulation (UWVF) [11, 12]. For details, see [31, 30].

Transducer excitations (amplitudes and phases) are chosen by using the specific optimization algorithm described in Publication IV. This algorithm is used to determine such excitations that the produced US field causes localized temperature elevation to a given location in tissue. Such excitations are computed for several chosen locations and these excitations are concatenated to form time-dependent excitations.

The evolution models are constructed by using the FEM and the implicit Euler method. The accurate and reduced model are constructed using different FE meshes and different time stepping in temporal discretization. The coefficients are estimated by using the adaptive estimation approach described in Section 2.4. The augmented state vector is $X_k^{\mathrm{A}} = (X_k, \kappa_k, \beta_k)$ where X_k is temperature represented in the FE basis and κ_k and β_k are vectors containing the values of κ and β in the regions in which these constants are unknown. Due to the large dimension of the measurement vector, the hybrid filter presented in Section 3.5 is used in this simulation.

Since the measurements are MR temperature images, the measurement operators in the state space models are chosen to be linear interpolation matrices from the computational meshes to the measurement grid. The synthetic temperature data for the simulation is computed using the FEM approximation which is constructed using very dense spatial and temporal discretization.

Results

In this simulation, the computational domain is chosen to be a 2D-domain representing a cross section of a cancerous breast. The domain is divided into four subdomains: Ω_{I} is a water bed that is needed for the practical setup, Ω_{II} is skin, Ω_{III} is the breast tissue and Ω_{IV} is the tumor. The thermal conductivity in the water layer Ω_{I} is assumed to be known. Furthermore, it is natural to assume that there is no perfusion in the subdomain Ω_{I}.

The energy of errors is distributed similarly as in the previous simulations. The time average of $\|\mathbb{E}[\epsilon_k^r]\|^2 + \operatorname{Tr}\operatorname{cov}(\epsilon_k^r) = 1.48$ which is again higher than $\operatorname{Tr}\Sigma_k^w = 0.017$. For the observation model the time average of $\|\mathbb{E}[\nu_k^r]\|^2 + \operatorname{Tr}\operatorname{cov}(\nu_k^r) = 13.8$ and $\operatorname{Tr}\Sigma_k^v = 16384$. Hence it seems that also in this case the effects of the approximation errors are significant only in the evolution model.

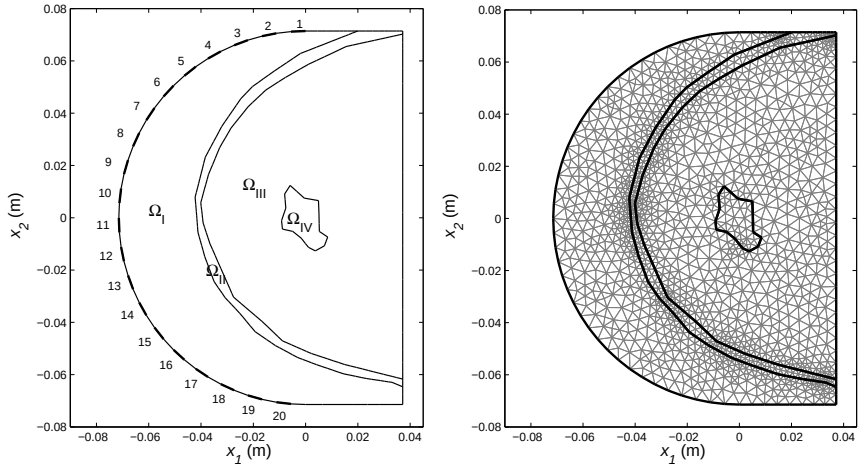

Figure 4.7: Left: the computational domain. The domain is divided into four subdomains Ω_{I}-Ω_{IV} in which physical parameters are assumed to be constant. Black lines on the left boundary represent ultrasound transducers (numbered 1,...,20). Right: the computational mesh consisting of 2965 elements and 1,533 nodes.

Two estimates are computed: an estimate computed using the enhanced error model and an estimate computed using the reduced model. In this case we cannot compute an estimate using the the accurate model since the model is computationally too demanding for the KF filter recursion. The computed estimates and error estimates are shown in Table 4.1. Similarly as in the previous simulation, the estimates and the error estimates are components of the filter estimate and the filter covariance corresponding to the coefficients κ and β. The results show that also in this simulation the use of the enhanced error model gives substantial improvement to the the accuracy of the estimates.

It is to be noted that the true error should not be much larger than the error estimates. For the estimate computed using the enhanced error model, the true error for each component is at the most 3.6 times higher than the computed error estimate representing the standard deviation, which in Gaussian cases would be considered as significant overestimation of the accuracy. Anyway, in this non-linear and thus non-Gaussian case, the significance of this difference is not so clear without information about the form of the distributions (that can be only obtained using Markov chain Monte Carlo type schemes). Furthermore, the linearizations in the derivation of the filter equations often cause that the error estimates are exaggerated. Nonetheless, this difference between estimated error and actual error is small compared to the estimates computed using the reduced model, in which the true error is throughout over 4 times larger than the error estimates.

Table 4.1: Computed estimates $\widehat{X}$ and error estimates $\widehat{\sigma}$. Two estimates are shown: the former estimate is computed using the enhanced error model and the latter by using the reduced error model.

		Enhanced error model			Reduced model		
	True	$\widehat{X}$	$\widehat{\sigma}$	True Error	$\widehat{X}$	$\widehat{\sigma}$	True Error
κ^{II}	0.650	0.597	0.025	0.053	0.567	0.020	0.083
κ^{III}	0.400	0.421	0.014	0.021	0.523	0.024	0.123
κ^{IV}	0.800	0.732	0.093	0.069	1.367	0.142	0.567
β^{II}	4524	6777	634	2253	2104	485	2420
β^{III}	3393	3283	82	110	4695	85	1302
β^{IV}	6409	6241	318	168	8951	360	2542

Chapter V

Conclusions and discussion

In this thesis we carried out the approximation error analysis for nonstationary inverse problems. We derived approximation error models to take into account errors related to discretizations and model reduction in linear and nonlinear state space estimation problems. The formalism allows us to take into account the errors due to both spatial and temporal discretization. We also derived modifications for the Kalman filter recursion to accommodate the approximation error models. Furthermore, we derived a version of the proposed method which is computationally more efficient in a situation in which the number of measurements is high compared to the dimension of the state vector. Finally, as applications we considered four different test cases in which the proposed approach was applied to take into account discretization errors in the evolution and observation models.

The proposed approach can be used in several industrial and medical applications. The approach allows us to use the approximative low dimensional model without compromising the accuracy of the estimates. The use of the approximative models is especially important in nonstationary inverse problem in which the constraints for the processing time are very tight. For example, in continuous monitoring or control in process tomography, the time between the measurements is of the order of milliseconds, within which time the Kalman filter recursion and possibly also the control has to be computed [63, 60]. This time would be too short for high-dimensional models. For the same reason, the optimal control based treatment planning cannot be carried out clinically yet.

In the simulations carried out in thesis, the approximation error approach provides a significant improvement to the accuracy of the estimates when compared to estimates computed using the Kalman filter recursion without taking into account approximation errors. Furthermore, the proposed approach provides error estimates which correspond well to the actual errors, which, however, is not the case when the approximation errors are not taken into account.

The computation of the statistics of the approximation error terms is often a computationally demanding task. For example, stochastic simulation using the high–dimensional accurate model is required and therefore the computation of a representative ensemble of samples may be very time-consuming. However, this task has to be carried out only once for each measurement system and it can be done prior any measurements are given. Furthermore, the high–dimensional model is not required in the solution of the estimation problem itself. While the filtering recursion is computed, the use of the proposed method

in the solution of the state estimation problem is computationally almost as heavy as the use of a small-dimensional model without the approximation error models.

The approximation error analysis can also be used to handle uncertainties caused by unknown model parameters. The basic idea of this treatment is similar to the approach used in this thesis. The corresponding approximation error models are derived for errors caused by the uncertainties in the unknown parameters, and the statistics of these errors can be determined, for example, by using similar sampling based methods. This kind of approach is used to handle the uncertainties caused by anisotropies in optimal tomography [27], and in hydrological process monitoring to handle uncertainties in the permeability field [45].

Summary of publications

I **Approximation Errors In Nonstationary Inverse Problems** (Inverse Problems and Imaging, 1:77-93, 2007).

This publication introduces an extension of the approximation error methods for nonstationary inverse problem. Firstly, the approximation error models are derived for linear state space estimation problems. Both the errors due to the model reduction and temporal integration are handled. Secondly, an extension of the Kalman filter recursion to accommodate the approximation error models is derived in this paper. For the numerical verification of the proposed approach, we consider a simple heat-equation problem, in which the temperature distribution in a one–dimensional rod is predicted from measurements taken at given points.

II **Discretization error in dynamical inverse problems: one-dimensional model case** (Journal of Inverse and Ill-Posed Problems, 15:365-386, 2007).

In this paper a further research of the study in [56, 57] is carried out. We consider nonstationary inverse problems in which the time evolution of the unknown is modelled by a stochastic partial differential equation. In this approach the induced stochastic initial value problem is solved using semigroups. This semigroup is then used to construct a state space representation for the system, in which the unknown state is an element of an infinite–dimensional vector space. The main purpose of this publication is to carry out a numerical implementation for the one–dimensional model problem presented in [56]. The state space representation for the problem is obtained using the results presented in [56, 57] and the estimation problem is solved using the filtering recursion presented in Publication I.

III **Approximation error analysis in nonlinear state estimation with an application to state-space identification** (Inverse Problems, 23:2141-2157, 2007).

This paper considers a nonlinear extension of the approximation error approach described in Publication I. An approximation error model are constructed for nonlinear state space models taking into account the model reduction and increased time stepping. Furthermore, the filtering recursion equations for the nonlinear approximation error model are derived. As an example, the identification of the heterogeneous coefficients of the 1D heat equation is considered.

IV **Determination of heterogeneous thermal parameters using ultrasound induced heating and MR thermal mapping** (Physics in Medicine and Biology, 51:1011–1032, 2006).

In this publication, the determination of heterogeneous thermal conductivity and perfusion of tissue is considered. We propose a method to determine the thermal properties by using ultrasound induced heating and magnetic resonance (MR) thermal imaging. The basic idea of this method is to inflict small temperature changes into tissue which are monitored by using MR scanner. The thermal properties are determined on the basis of these measurements using the maximum a posteriori estimation scheme. Furthermore, an approach to choose amplitudes and phases of ultrasound transducers for the determination procedure is also considered.

V **Model reduction in state identification problems with an application to determination of distributed thermal parameters** (Applied Numerical Mathematics, in review).

In this paper model reduction errors in state space identification problems are consid-

ered. We treat state space identification problems as adaptive estimation problems and use the previous results with the resulting augmented state space form. Furthermore, we derive a computationally efficient form of the filtering recursion for situation in which the number of measurements is high compared to the dimension of the state space. As an application, we apply the approach to the determination of heterogeneous thermal parameters of tissue. The method to determine the thermal properties is similar to Publication IV with an exception that in this publication the problem is treated as a state identification problem.

Author's contribution

All publications are result of the joint work with co-authors. The author has been the principal writer in Publications I, III, IV and V. In these publications, the author has been responsible in developing the methods presented the publications, has carried out all the implementations of numerical simulations and computed results in the Matlab® platform. As an exception, the computational domain and the ultrasound fields in Publications IV and V are previously created by co-authors in [47]. In Publication II the writing task has been divided equally among the authors of this article. Furthermore, the author has carried out the numerical simulation and computed the results presented in this publication.

REFERENCES

[1] L. Aggoun and R. Elliott. *Measure Theory and Filtering.* Cambridge University Press, 2004.

[2] B.D.O. Anderson and J.B. Moore. *Optimal filtering.* Prentice-Hall, inc, 1979.

[3] D.P. Anhalt, K. Hynynen, and R.B. Roemer. Patterns of changes of tumour temperatures during clinical hyperthermia: implications for treatment plannin, evaluation and control. *International Journal of Hyperthermia*, 11(3):425–436, 1995.

[4] A.C. Antoulas. *Approximation of Large-Scale Dynamical Systems.* Advances in Design and Control 6. Society for Industrial and Applied Mathematic, 2005.

[5] S.R. Arridge, J.P. Kaipio, V. Kolehmainen, M. Schweiger, E. Somersalo, T. Tarvainen, and M. Vauhkonen. Approximation errors and model reduction with an application in optical diffusion tomography. *Inverse Problems*, 22(1):175–196, 2006.

[6] A.V. Balakrishnan. *Elements of State Space Theory.* Optimization Software, 1983.

[7] A.V. Balakrishnan. *Kalman Filtering Theory.* Optimization Software, 1984.

[8] BC components. *Datasheet 2322 640 3/4/6. NTC termistors*, Septemper 2001.

[9] A.B. Bhatia. *Ultrasound Absorption: An Introduction to the Theory of Sound Absorption and Dispersion in Gases, Liquids, and Solids.* Oxford University Press, 1967.

[10] P.J. Brockwell and R.A. Davis. *Time Series: Theory and Methods.* Springer-Verlag, 1991.

[11] O. Cessenat. *Application d'une nouvelle formulation variationelle des equations d'ondes harmonigues, Problemes de Helmholtz 2D et de Maxwell 3D.* PhD thesis, Paris IX Dauphine, 1996.

[12] O. Cessenat and B. Despres. Application of an ultra-weak variational formulation of elliptic PDEs to the two-dimensional Helmholtz problem. *SIAM Journal of Numerical Analysis*, 35(1):255–299, 1998.

[13] J.Y. Chapelon, M. Ribault, A. Birer, F. Vernier, R. Souchon, and A. Gelet. Treatment of localised prostate cancer with transrectal high intensity focused ultrasound. *European Journal of Ultrasound*, 9:31–38, 1999.

[14] H.L. Cheng and D.B. Plewes. Tissue thermal conductivity by magnetic resonance thermometry and focused ultrasound heating. *Journal of Magnetic Resonance Imaging*, 16(5):598–609, 2002.

[15] A. Doucet, N. de Freitas, and N. Gordon. *Sequential Monte Carlo Methods in Practice*. Statistics for Engineering and Information Science. Springer-Verlag, NY, 2001.

[16] F.A. Duck, A.C. Baker, and H.C. Starritt. *Ultrasound in Medicine*. Institute of Physics Publishing, 1998.

[17] R.M. Dudley. *Real Analysis and Probability*. Cambridge University Press, 2002.

[18] J. Durbin and S.J. Koopman. *Time Series Analysis by State Space Methods*. Oxford University Press Inc., 2001.

[19] B. Erdmann, J. Lang, and M. Seebass. Optimization of temperature distributions for regional hyperthermia based on a nonlinear heat transfer model. *K. Diller (ed.), Biotransport: Heat and Mass Transfer in Living Systems, Annals of the New York Academy of Sciences*, 858:36–46, 1998.

[20] G. Evensen. Sequential data assimilation with a non-linear quasigeostrophic model using monte carlo methods to forecast error statistics. *Journal of Geophyscal Research*, 99(C5):10143–10162, 1994.

[21] D.C. Fraser. A new technique for the optimal smoothing of data. Technical report, M.I.T. Instrumentation Lab, January 1967. Report T-474.

[22] J.A. Goldstein. *Semigroups of Linear Operators And Applications*. Oxford University press, 1985.

[23] G.H. Golub and C.F. van Loan. *Matrix Computations*. The Johns Hopkins University Press, 1989.

[24] G. Goodwin and R. Payne. *Dynamic System Identification*. Academic Press, 1977.

[25] M.S. Grewal and A.P. Andrews. *Kalman filtering: Theory and Practice*. Prentice Hall, New Jersey, 1993.

[26] J. Heino. Approaches for modelling and reconstruction in optical tomography in the presence of anisotropies. Doctoral dissertation, Helsinki University of Technology, 2005.

[27] J. Heino and E. Somersalo. A modelling error approach for the estimation of optical absroption in the presence of anisotropies. *Physics in Medicine and Biology*, 49:4785–4798, 2004.

[28] E. Hille and R.S. Phillips. *Functional Analysis and Semi-Groups*. AMS, 1957.

[29] R.A. Horn and C.R. Johnson. *Matrix Analysis*. Cambridge University Press, 1985.

[30] T. Huttunen. *The ultraweak variational formulation for ultrasound transmission problems*. PhD thesis, University of Kuopio, February 2004.

[31] T. Huttunen, P. Monk, and J.P. Kaipio. Computational aspects of the ultraweak variational formulation. *Journal of Computational Physics*, 182:27–46, 2002.

[32] K. Hynynen, W.R. Freund, H.E. Cline, A.H. Chung, R.D. Watkins, J.P. Vetro, and F.A. Jolesz. A clinical, noninvasive, MR imaging-monitored ultrasound surgery method. *Radiographics*, 16(1):185–195, January 1996.

[33] Y. Ishihara, A. Calderon, H. Watanabe, K. Okamoto, Y. Suzuki, K. Kuroda, and Y. Suzuki. A precise and fast temperature mapping using water proton chemical

shift. *Magnetic Resonance in Medicine*, 34:814–823, December 1995.

[34] J.P. Kaipio and E. Somersalo. Nonstationary inverse problems and state estimation. *Journal of Inverse and Ill-Posed Problems*, 7:273–282, 1999.

[35] J.P. Kaipio and E. Somersalo. *Statistical and Computational Inverse Problems*. Applied Mathematical Sciences 160, Springer-Verlag, 2004.

[36] J.P. Kaipio and E. Somersalo. Statistical inverse problems: Discretization, model reduction, and inverse crimes. *Journal of Computational and Applied Mathematics*, 198:493–504, 2007.

[37] R.E. Kalman. A new approach to linear filtering and prediction problems. *Journal of Basic Engineering Transactions of the ASME (Series D)*, 82:35–45, 1960.

[38] R.E. Kalman and R.S. Bucy. New results in linear filtering and prediction theory. *Journal of Basic Engineering*, 83D:35–45, 1961.

[39] I. Karatzas and S. E. Shreve. *Brownian Motion and Stochastic Calculus*. Graduate Texts in Mathematics. Springer-Verlag, NY, 2nd edition, 1991.

[40] H. Kunita. *Stochastic Flows and Stochastic Differential Equations*. Cambridge University Press, 1990.

[41] S.W. Lang. Bounds from noisy linear measuremements. *IEE Transactions on Information Theory*, IT-31(4):498–508, 1985.

[42] S. Lasanen. *Discretizations of Generalized Random Variables with Applications to Inverse Problems*. PhD thesis, University of Oulu, Annales Academiae Scientiarum Fennicae, Mathematica Dissertationes 130, 2002.

[43] M. Lassas and S. Siltanen. Can one use total variation prior for edge preserving bayesian inversion. *Inverse Problems*, 20:1537–1564, 2004.

[44] A. Lehikoinen, S. Finsterle, A. Voutilainen, L.M. Heikkinen, M. Vauhkonen, and J.P. Kaipio. Approximation errors and truncation of computational domains with application to geophysical tomography. *Inverse Problems and Imaging*, 1(2):371–389, 2007.

[45] A. Lehikoinen, J.M.J. Huttunen, A. Voutilainen, S. Finsterle, M.B. Kowalsky, and J. P. Kaipio. A new dynamic inversion approach for hydrological process monitoring. *Water resources research, to be submitted*, 2007.

[46] I.J. Maddox. *Elements Of Functional Analysis*. Cambridge University Press, 1988.

[47] M. Malinen, S.R. Duncan, T. Huttunen, and J.P. Kaipio. Feedforward and feedback control of ultrasound surgery. *Applied Numerical Mathematics*, 56:55–79, 2006.

[48] M. Malinen, T. Huttunen, and J.P. Kaipio. Thermal dose optimization method for ultrasound surgery. *Physics in Medicine and Biology*, 48:745–762, 2003.

[49] N. McDannold, K. Hynynen, D. Wolf, G. Wolf, and F.A. Jolesz. MRI evaluation of thermal ablation of tumors with focused ultrasound. *Journal of Magnetic Resonance Imaging*, 8:91–100, 1998.

[50] B. Øksendal. *Stochastic Differential Equations*. Springer-Verlag, 1998.

[51] D.L. Parker, V. Smith, P. Sheldon, L.E. Crooks, and L. Fussell. Temperature distribution measurements in two-dimensional NMR imaging. *Medical Physics*, 10:321–325, 1983.

[52] A. Pazy. *Semigroups of Linear Operators and Applications to Partial Differential Equations*. Springer-Verlag, 1992.

[53] H. H. Pennes. Analysis of tissue and arterial blood temperatures in the resting human forearm. *Journal of Applied Physiology*, 1:93–122, 1948.

[54] A.D. Pierce. *Acoustics: An introduction to its physical principles and applications*. Acoustical Society of America, 1991.

[55] P. Piiroinen. *Statistical Measurements, experiments and applications*. PhD thesis, University of Helsinki, Annales Academiae Scientiarum Fennicae, Mathematica Dissertationes 143, 2005.

[56] H.-K. Pikkarainen. A mathematical model for electrical impedance process tomography. Doctoral dissertation, Helsinki University of Technology, 2005.

[57] H.-K. Pikkarainen. State estimation approach to nonstationary inverse problems: discretization error and filtering problem. *Inverse Problems*, 22:365–379, 2006.

[58] G. Da Prato and J. Zabczyk. *Stochastic Equations in Infinite Dimensions*. Cambridge University Press, 1992.

[59] W. Rudin. *Functional Analysis*. McGraw-Hill, 2nd edition, 1991.

[60] A.R. Ruuskanen, A. Seppänen, S. Duncan, E. Somersalo, and J.P. Kaipio. Using Process Tomography as a Sensor for Optimal Control. *Applied Numerical Mathematics*, 56:37–54, 2006.

[61] N.T. Sanghvi, R.S. Foster, R. Bihrle, R. Casey, T. Uchida, M.H. Phillips, J. Syrus, A.V. Zaitsev, K.W. Marich, and F.J. Fry. Noninvasive surgery of prostate tissue by high intensity focused ultrasound: an updated report. *European Journal of Ultrasound*, 9:19–29, 1999.

[62] A. Seppänen, M. Vauhkonen, E. Somersalo, and J.P. Kaipio. State space models in process tomography - approximation of state noise covariance. *Inverse Problems and Engineering*, 9:561–585, 2001.

[63] A. Seppänen, M. Vauhkonen, P. J. Vauhkonen, E. Somersalo, and J.P. Kaipio. State estimation with fluid dynamical evolution models in process tomography – an application with impedance tomography. *Inverse Problems*, 17:467–484, 2001.

[64] S. Shreve. Stochastic calculus and finance. Lecture notes, http://www-2.cs.cmu.edu/∼chal/shreve.html, July 1997.

[65] P.B. Stark. Inference in infinite-dimensional inverse problems: Discretization and duality. *Journal of Geophysical Research*, 97(B10):14055–14082, 1992.

[66] G. Vallancien, M. Harouni, B. Guilloneau, B. Veillon, and J. Bougaran. Ablation of superficial bladder tumors with focused extracorporeal pyrotherapy. *Urology*, 47:204–207, 1996.

[67] A. Vanne and K. Hynynen. MRI feedback temperature control for focused ultrasound surgery. *Physics in Medicine and Biology*, 48:31–43, 2003.

[68] A.G. Visioli, I.H. Rivens, G.R. ter Haar, A. Horwich, R.A. Huddart, E. Moskovic, A. Padhani, and J. Glees. Preliminary results of phase I dose escalation clinical trial using focused ultrasound in the treatment of localised tumours. *European Journal of Ultrasound*, 9:11–18, 1999.

[69] J.A. Vrugt, C.G.H. Diks, H.V. Gupta, W. Bouten, and J.M. Verstrated. Improved treatment of uncertainty in hydrological modelling: Combining the strength of global optimization and data assimilation. *Water Resources Research*, 41, W01017, doi:10.1029/2004WR003059, 2005.

[70] N. Vykhodtseva, V. Sorrentino, F.A. Jolesz, R.T. Bronson, and K. Hynynen. MRI detection of the thermal effects of focused ultrasound in the brain. *Ultrasound in Medicine and Biology*, 26(5):871–880, 2000.

[71] F.M. Waterman, L. Tupchong, R.E. Nerlinger, and J. Matthews. Blood flow in human tumors during local hyperthermia. *Int J Radiat Oncol Biol Phys*, 20(6):1255–62, June 1991.

[72] M. West and J. Harrison. *Bayesian Forecasting and Dynamic Models*. Springer Series in Statistics. Springer-Verlag, NY, second edition, 1999.

[73] D. Williams. *Probability with Martingales*. Cambridge University Press, 1991.

[74] A.E. Worthington, J. Trachtenberg, and M.D. Sherar. Ultrasound properties of human prostate tissue during heating. *Ultrasound in Medicine & Biology*, 28(10):1311–1318, October 2002.

Kuopio University Publications C. Natural and Environmental Sciences

C 208. Anttonen, Mikko J. Evaluation of Means to Increase the Content of Bioactive Phenolic Compounds in Soft Fruits.
2007. 93 p. Acad. Diss.

C 209. Pirkanniemi, Kari. Complexing agents: a study of short term toxicity, catalytic oxidative degradation and concentrations in industrial waste waters.
2007. 83 p. Acad. Diss.

C 210. Leppänen, Teemu. Effect of fiber orientation on cockling of paper.
2007. 96 p. Acad. Diss.

C 211. Nieminen, Heikki. Acoustic Properties of Articular Cartilage: Effect of Structure, Composition and Mechanical Loading.
2007. 80 p. Acad. Diss.

C 212. Tossavainen, Olli-Pekka. Shape estimation in electrical impedance tomography.
2007. 64 p. Acad. Diss.

C 213. Georgiadis, Stefanos. State-Space Modeling and Bayesian Methods for Evoked Potential Estimation.
2007. 179 p. Acad. Diss.

C 214. Sierpowska, Joanna. Electrical and dielectric characterization of trabecular bone quality.
2007. 92 p. Acad. Diss.

C 215. Koivunen, Jari. Effects of conventional treatment, tertiary treatment and disinfection processes on hygienic and physico-chemical quality of municipal wastewaters.
2007. 80 p. Acad. Diss.

C 216. Lammentausta, Eveliina. Structural and mechanical characterization of articular cartilage and trabecular bone with quantitative NMR .
2007. 89 p. Acad. Diss.

C 217. Veijalainen, Anna-Maria. Sustainable organic waste management in tree-seedling production.
2007. 114 p. Acad. Diss.

C 218. Madetoja, Elina. Novel process line approach for model-based optimization in papermaking.
2007. 125 p. Acad. Diss.

C 219. Hyttinen, Marko. Formation of organic compounds and subsequent emissions from ventilation filters.
2007. 80 p. Acad. Diss.

C 220. Plumed-Ferrer, Carmen. Lactobacillus plantarum: from application to protein expression.
2007. 60 p. Acad. Diss.

C 221. Saavalainen, Katri. Evaluation of the mechanisms of gene regulation on the chromatin level at the example of human hyaluronan synthase 2 and cyclin C genes.
2007. 102 p. Acad. Diss.

C 222. Koponen, Hannu T. Production of nitrous oxide (N□O) and nitric oxide (NO) in boreal agricultural soils at low temperature.
2007. 102 p. Acad. Diss.